

The fundamental properties of galaxies and a new galaxy classification system

Christopher J. Conselice[★]

University of Nottingham, School of Physics & Astronomy, Nottingham NG7 2RD

Accepted 2006 September 27. Received 2006 September 22; in original form 2006 June 27

ABSTRACT

We present in this paper a new three-dimensional galaxy classification system designed to account for the diversity of galaxy properties in the nearby universe. To construct this system we statistically analyse a sample of $>22\,000$ galaxies at $v < 15\,000 \text{ km s}^{-1}$ ($z < 0.05$) with Spearman rank and principal-component analyses (PCAs). Fourteen major galaxy properties are considered, including: Hubble type, size, colour, surface brightness, magnitude, stellar mass, internal velocities, H I gas content and an index that measures dynamical disturbances. We find, to a high degree, that most galaxy properties are correlated, with in particular Hubble type, colour and stellar mass all strongly related. We argue that this tight three-way correlation is a result of evolutionary processes that depend on galaxy mass, as we show that the relation between colour and mass is independent of Hubble type. Various PCAs reveal that most of the variation in nearby galaxy properties can be accounted for by eigenvectors dominated by (i) the scale of a galaxy, such as its stellar mass, (ii) the spectral type and (iii) the degree of dynamical disturbances. We suggest that these three properties: mass, star formation and interactions/mergers are the major features that determine a galaxy's physical state, and should be used to classify galaxies. As shown by Conselice et al., these properties are measurable within the CAS (concentration, asymmetry, clumpiness) structural system, thus providing an efficient mechanism for classifying galaxies in optical light within a physical meaningful framework. We furthermore discuss the fraction and number density of galaxies in the nearby universe as a function of Hubble type, for comparison with higher redshift populations.

Key words: galaxies: evolution – galaxies: formation – galaxies: structure.

1 INTRODUCTION

Galaxies as distinct stellar, gaseous and dark matter units have dozens of properties measurable by a variety of techniques from gamma-ray to radio wavelengths. Some of the most basic properties include: spectral energy distributions, spectral line properties, sizes, internal velocities, structural features and morphologies. From these observable quantities we can derive additional physical information, such as stellar, gaseous and total masses, metallicities, the current and past star formation rates and the fraction of light in various structural components. Each of these features reveals potentially important clues for how galaxies, including their gas content and dark matter haloes, were created and have evolved. These properties are also interrelated through well-known scalings, such as the colour–magnitude relation (e.g. Sandage & Visvanathan 1978), the size–magnitude relation (e.g. Romanishin 1986), the Tully–Fisher relation (Tully & Fisher 1977), and the Fundamental Plane (Djorgovski & Davis 1987; Dressler et al. 1987). These correlations

all describe the scaling of structural features of normal galaxies with each other, or with the internal kinematics of galaxies.

It is however not yet clear what the most basic evolutionary processes and galaxy observables are, and whether or not well-known relations between galaxy parameters capture essential galaxy features. Is there a single, or a group of processes responsible for the diversity of galaxies? Although it is widely known that physical properties vary along the Hubble sequence, galaxies within a Hubble type have a large range of sizes, colours, surface brightnesses, masses and so on. Perhaps there is an alternative way to classify galaxies based on the properties responsible for driving evolution. One goal of this paper is determining what physical features of galaxies are the best for classification purposes. Currently it is assumed by many that the optical morphology of a galaxy provides this classification, either in the form of a Hubble type, or through quantitative methods. However, there is no *a priori* reason that optical morphologies should reveal information needed to classify galaxies into a meaningful system.

We utilize 14 properties of 22 121 galaxies in the nearby universe to address this problem. We begin our analysis with the hypothesis that our 14 measurable features provide the basic physical

[★]E-mail: conselice@nottingham.ac.uk

information needed to fully characterize nearby galaxies. We analyse these measurables through statistical methods, such as Spearman rank and principal-component analyses (PCAs), to determine which observables are the most fundamental for classifying galaxies. We demonstrate that at a fundamental level many measured properties of galaxies correlate with each other. For example, scale features correlate strongly, and Hubble types correlate with many properties, including colour and stellar mass. We argue that this correlation is the reason that Hubble types have been successful in describing the nearby galaxy population.

We further show through PCA that most of the variation in galaxy properties can be accounted for by three eigenvectors (EVs) dominated by scale (e.g. mass), the presence of star formation, and the degree of recent interaction/merger activity. As a result, our main conclusion is that these three features are needed to understand the current and past evolutionary state of a galaxy. We further argue that galaxy mass, star formation and mergers/interactions are responsible for the diversity in the galaxy population in the nearby universe, and should be used to construct a galaxy classification system.

This paper is a more general companion, and in some ways a prequel, to the quantitative CAS (concentration, asymmetry, clumpiness) structural analysis paper presented in Conselice (2003). In Conselice (2003) we created a new quantitative way to classify galaxies under the assumption that mass, star formation, and recent mergers were the critical properties for understanding galaxies. We now show that this assumption is justifiable through our statistical analysis of $>22\,000$ nearby galaxies. Conselice (2003) furthermore developed a quantitative and reproducible method for retrieving this information through the optical light of galaxies.

The outline of this paper is as follows. In Section 2 we give a summary of the physical features, and formation histories of various types of galaxies we study. Section 3 describes our galaxy sample, and the properties we use to characterize each system. Section 4 gives a detailed description of the nearby galaxy population, including the relative numbers and number densities of various morphological types. Section 5 presents our statistical analysis of our sample, while Section 6 utilizes this information to produce a new physical classification system, and Section 7 is a summary. For distance measurements we use a Hubble constant of $H_0 = 70 \text{ km s}^{-1} \text{ Mpc}^{-1}$, unless otherwise noted.

2 NEARBY GALAXY TYPES AND THEIR POSSIBLE FORMATION HISTORIES

There are a few generally agreed upon major nearby basic galaxy types, generally classified according to morphology, whose properties and range of possible formation histories are becoming well understood. These types are: ellipticals, spirals, lenticulars, dwarf spheroidals/ellipticals, low surface brightness (LSB) galaxies, irregulars and mergers, which we review below. These groups can, but do not necessarily include, other types of galaxies such as starbursting systems (e.g. ultraluminous infrared galaxies, ULIRGs), galaxies with active galactic nuclei, AGNs (e.g. quasars, radio galaxies, etc.).

Most *ellipticals*, particularly those in clusters, contain old stellar populations that likely formed early in the universe (Kuntschner & Davies 1998). Many of these galaxies are thought to form by the mergers of smaller galaxies (Barnes & Hernquist 1992), or from a rapid collapse of non-rotating gas (van Albada 1982). The merger idea for the origin of ellipticals is currently popular, with both indirect and direct supporting evidence (e.g. Schweizer & Seitzer 1988; Conselice 2006).

Spiral galaxies are a mixed galaxy class, but all generally show evidence of recent star formation and past merger/accretion activity (e.g. Kennicutt 1998; Zaritsky & Rix 1997). The stellar populations in spirals are also younger, on average, than those found in giant ellipticals (e.g. Trager et al. 2000).

The *lenticular class* (S0s) are disc-like galaxies without the presence of strong spiral arms, star formation, obvious dust, or gas usually associated with spirals and other star-forming galaxies. S0 galaxies are usually found in galaxy clusters (Dressler 1984), but can also exist in the field (e.g. van den Bergh 1997). It has been suggested since Spitzer & Baade (1951) that S0s originate from spirals due to environmental effects. Evidence for this includes spirals in nearby clusters that are highly depleted in gas (Haynes & Giovanelli 1986), and might be evolving into S0 galaxies.

Dwarf ellipticals (dE), the most common type of galaxy in the nearby universe, are almost always located in dense environments such as galaxy clusters and groups (Ferguson & Binggeli 1994). These objects resemble ellipticals due to their symmetric structure, and elliptical isophotes, although they differ in several significant properties, such as containing different light profiles, and how they follow scaling relations (e.g. Wirth & Gallagher 1984; Graham & Guzman 2003). These objects likely have several formation mechanisms, including a primordial origin and evolution from stripped galaxies (Conselice, Gallagher & Wyse 2001, 2003c).

LSB galaxies are one of the last major class of galaxies discovered to date (Disney 1976). These objects come in many shapes and sizes, but generally mimic the Hubble sequence in terms of bulge-to-disc ratios, but at a much lower surface brightness, at $\mu > 24 \text{ mag arcsec}^{-2}$ (see Impey & Bothun 1997). It has been suggested from several pieces of observational evidence that LSB galaxies have had few, if any, major merging or interaction events with other galaxies, and are found in relative isolation (e.g. Knezeck 1993; Mo, McGaugh & Bothun 1994). LSB galaxies therefore potentially represent a class of objects formed mostly through the collapse of gas, with gradual and continual ongoing star formation, with few interactions throughout their history.

Irregulars are typically smallish star-forming galaxies that often lack a distinct spiral structure. For our purposes, irregulars include dwarf irregulars, blue compact dwarfs and classical irregulars such as NGC 4449. Star formation dominates the appearance and evolution of these small, but common, galaxies that have a wide range of surface brightnesses (see Gallagher & Hunter 1984, for a review). They are also the bluest type of non-interacting galaxy known (Huchra 1977). A large amount of attention has been spent studying the dIrr members of the local group, although these objects also exist in clusters (e.g. Binggeli, Sandage & Tammann 1985; Gallagher & Hunter 1986).

Finally, *interacting and merging galaxies*, while rare in the nearby universe, were much more common in the distant past when roughly half of all massive galaxies were undergoing major mergers (e.g. Conselice et al. 2003a,b). Mergers are likely a critically important galaxy formation/evolution process especially if the first galaxies were all of low mass. Mergers are also observationally more common at earlier times (e.g. Conselice et al. 2003a; Bundy et al. 2004; Lin et al. 2004; Pope et al. 2005).

3 NEARBY GALAXY ANALYSIS

3.1 RC3 sample and data

The sample of galaxies with which we performed our statistical analyses were taken from galaxies in the Third Reference Catalogue

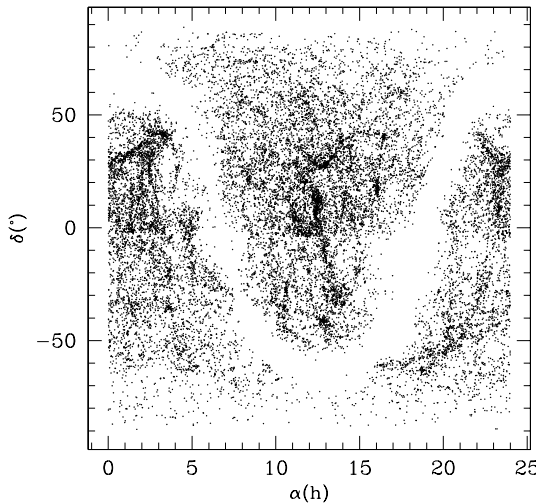


Figure 1. The spatial distribution of the galaxies used for our statistical study of galaxy populations and their properties. The U-shaped gap is the galactic plane, and the structure at the centre constitutes the Virgo supercluster.

of Bright Galaxies (hereafter RC3; de Vaucouleurs et al. 1991). These RC3 galaxies were chosen based on their size (>1 arcmin), apparent magnitude $B_T < 15.5$ and radial velocity ($v < 15\,000 \text{ km s}^{-1}$), although the catalogue is supplemented by objects that met only one of these criteria. This catalogue is however inhomogeneous, which we deal with in several ways, described in the following analysis. For each galaxy we culled from the literature, or derive, the following features. Our total sample consists of 22 121 galaxies distributed across the sky as shown in Fig. 1. The average galaxy in our sample is at L_* , and its average galaxy colour is $(B - V)_0 = 0.66$.

(i) T-type (T): The mean de Vaucouleurs (1959) T-type is an expression of the gross morphology of a galaxy. The T-type values we used are means for each galaxy, computed from a variety of sources (RC3). These T-types can be equated with Hubble types as: -6 through -4 are ellipticals, -3 through -1 are S0s and 0 through 9 are S0/a, Sa, Sab, Sb, Sbc, Sc, Scd, Sd, Sdm and Sm, respectively. The RC3 is the largest eye-ball-estimated morphological catalogue to date.

(ii) Size (R): The sizes of each galaxy is computed from the isophotal major axis diameter (D_{25}) measured in arcminutes and converted into kpc by using the distance modulus (DM) for each galaxy. While Petrosian radii, or a radius which does not use isophotes, is more ideal, the effects of using an isophotal radii for these nearby systems is minor.

(iii) Mean effective surface brightness ($\langle\mu\rangle_e$): The mean effective surface brightness is the surface brightness within the half-light radius of each galaxy. This parameter, effectively combines the size and magnitude of a galaxy and gives us a rough idea of the projected density of stars.

(iv) $(U - B)_0$ and $(B - V)_0$ colours: These are photometrically determined colour indices corrected for galactic and internal extinction. We used these indices as a measure of the average luminosity weighted age of stars in galaxies, although for older (> 6 Gyr) stellar populations these colours can be dominated by metallicity effects (e.g. Worthey 1994).

(v) $\text{H}\alpha$ linewidths (W_{20} and W_{50}): The $\text{H}\alpha$ linewidths at the 20 and 50 per cent of the maximum level in the 21-cm line profile.

(vi) $\text{H}\alpha$ linewidth ratio ($I = W_{20}/W_{50}$): We used this number, based on the arguments in Conselice, Bershady & Gallagher (2000b) as a measure of the importance of recent interactions and mergers. Values of $I > 1.5$ are interpreted as systems that have recently undergone interactions or merger with other galaxies. We discuss this index in more detail in Section 3.2 and Conselice et al. (2000b).

(vii) Central velocity dispersion (V_S): This is usually only defined for early-type galaxies, and V_S^2 times a size can be used as a measure of early-type galaxy mass.

(viii) $\text{H}\alpha$ line index ($H\alpha$): It is defined as $m_{21} = 16.6 - 2.5 \log S_H$, where S_H is the flux of the $\text{H}\alpha$ line measured in units of W m^{-2} . We further subtract this value by the DM to obtain physical quantities that are independent of distance. We use the $\text{H}\alpha$ line index as a measure of the cold neutral gas content in a galaxy.

(ix) Far-infrared index (FIR): It is defined in a similar manner as the $\text{H}\alpha$ line index ($H\alpha$), as $m_{\text{FIR}} = -20 - 2.5 \log(\text{FIR}) - \text{DM}$, where $\text{FIR} = 1.26[2.58 \times f_\nu(60 \mu\text{m}) + f_\nu(100 \mu\text{m})]$, and $f_\nu(60 \mu\text{m})$ and $f_\nu(100 \mu\text{m})$ are the total flux densities in the IRAS 60 and 100 μm bands (RC3) and where DM is the DM of the galaxy.

(x) Luminosity class (λ): λ is the van den Bergh (1966) DDO, morphologically determined luminosity class index, which have been extended to fainter magnitudes in the RC3. The luminosity class values we used are weighted averages, just as the T-types, and have values that range from $\lambda = 1$ to 11 with higher λ values for fainter galaxies.

(xi) The maximum rotational velocity (V_{\max}): V_{\max} is defined as the maximum rotational velocity of a galaxy, as measured from $\text{H}\alpha$ or $\text{H}\beta$ rotation curve profiles. The size of a disc galaxy times V_{\max}^2 is sometimes used as a measure of its total mass.

(xii) The absolute B -band magnitude (M_B).

(xiii) The environmental galaxy density ρ : This is defined as the number of galaxies within 3 Mpc and $< 1000 \text{ km s}^{-1}$ of each galaxy in our catalogue. To avoid severe incompleteness for faint galaxies, we only compute this number for bright galaxies with $M_B < -20$ and at declinations $\delta > -30$.

(xiv) Galaxy stellar mass: Stellar masses for our sample were computed by deriving the stellar mass-to-light ratio (M/L) in the B band using the $(B - V)$ versus M/L relation discussed in Bell et al. (2003), using their ‘diet’ Salpeter initial mass function. There is a general correlation between stellar M/L and colour, such that bluer colours have lower stellar M/L. We used this relation, and the measured $(B - V)_0$ colours for our galaxies to derive the M/L in the B band for our sample. We then compute stellar masses by multiplying the luminosity in the B band for each galaxy by its derived stellar M/L.

Not all galaxies in our sample have each of these parameters measured, therefore when comparing different parameters we often had to use a subset of the data. We also associate with these parameters an error that reflects the variation in the measured values.

3.2 The galaxy interaction/merger index (I)

The galaxy interaction and merger index, I , defined by the ratio of the width of the $\text{H}\alpha$ line at 20 and 50 per cent of maximum (property VI in Section 3.1) is used in this paper as the principle indicator for finding galaxies undergoing mergers and interactions. It is a dynamical indicator and has been used at least once before for this purpose in Conselice et al. (2000b). However, it is not a standard galaxy measure and it is worth describing it, and the galaxies it selects, in more detail.

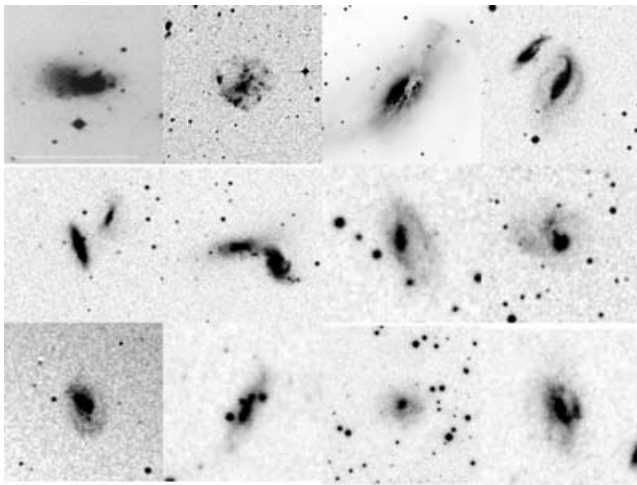


Figure 2. Examples of galaxies within our sample, mostly taken from the DSS, which have large 20–50 per cent H I linewidth ratios, I . As can be seen galaxies in interactions, in pre-mergers and post-mergers will all produce high H I linewidth ratios.

The idea behind its use is that a normal galaxy with H I, will present a regular H I profile that is relatively narrow, or at least does not significantly change shape. If a galaxy is interacting or merging, and H I gas is disturbed by these dynamical events then the H I profile will have a shallow rise, or will have wings. This leads to higher values of $I = W_{20}/W_{50}$. Conselice et al. (2000b) show that the I index correlates well with the asymmetry parameter, such that galaxies with very large asymmetries due to merging have large I values.

However, beyond the sample in Conselice et al. (2000b), this index has not been tested to determine its success rate in finding merging galaxies. To understand this better we examined the literature and Digitized Sky Survey (DSS) imaging for several hundred systems with $I > 2$. What we found was a diversity of galaxy morphology, from spirals and obvious mergers, to galaxies classified as S0s/ellipticals. However, it was nearly always the case that a system with a regular apparent morphology was in a galaxy pair, such that it is likely involved in an interaction with another galaxy. Examples of the optical morphology of the high- I systems taken from the NASA/IPAC Extragalactic Database (NED) and the DSS are shown in Fig. 2. It is clear from these images that the I indicator is a more sensitive probe than the asymmetry index (Conselice 2003), which is designed to find galaxies that have already merged. It appears that the I index will become large during an interaction as well as throughout the merger of two galaxies. There is however some contamination from non-interacting galaxies into our high- I sample, as might be expected. This rate is however low, and does not affect our results, as it is only at the 5 per cent level. Much of this contamination seems to arise from edge-on disc galaxies.

4 NEARBY GALAXY PROPERTIES

Our primary goal using our large sized-limited sample of nearby galaxies with morphologies is determining the strongest correlations between measurable parameters (Section 5). Before doing this, we examine the nearby galaxy population, its overall distribution of properties, and how each relates to morphological type. One purpose for this is having a well-defined morphological census of nearby galaxies to compare with more distant samples studied with the *Hubble Space Telescope* (*HST*).

4.1 Galaxy stellar mass and spectromorphology at $z \sim 0$

As the *HST* can now reveal the morphological properties, and stellar masses of thousands of galaxies at $z > 0.5$ (Conselice et al. 2004; Bundy, Ellis & Conselice 2005; Conselice, Blackburne & Papovich 2005a; Papovich et al. 2005), direct morphological and stellar mass comparisons with the $z = 0$ galaxy population are now possible (e.g. van den Bergh, Cohen & Crabbe 2001; Conselice et al. 2005a,b). It is thus desirable to determine the morphological distribution of galaxies at $z \sim 0$ and how these relate to stellar masses and colours.

We first calculate some basic spectromorphological properties of nearby galaxies, including how stellar masses relate to morphology at $z \sim 0$. Our catalogue of 22 121 RC3 galaxies is however inhomogeneous, particularly for LSB systems. As Fig. 3 shows, we sample fainter galaxies at lower radial velocities, implying we are incomplete at fainter magnitudes. To partially overcome the incompleteness of our catalogue, we limit our morphological statistical analyses to systems which have $M_B < -20$ and $v < 10 000 \text{ km s}^{-1}$ ($z \sim 0.033$, 133 Mpc) (shown by the lines in Fig. 3). When investigating fainter galaxies with $M_B < -18$, we limits our analyses to objects with velocities $v < 3000 \text{ km s}^{-1}$ ($z \sim 0.01$, 40 Mpc).

In addition to the $M_B < -20$ and $v < 10 000 \text{ km s}^{-1}$ cut, we furthermore only consider galaxies between declination $-50 < \delta < 50$, and take into account the incompleteness of the galaxy distribution due to the Milky Way (Fig. 1) when calculating total number densities. Note that these number densities are based on the RC3 selection, and are not complete in any sense. Our densities however generally agree well with the densities derived from the morphological-type specific Schechter functions published in Marzke et al. (1998) and Nakamura et al. (2003). We investigate the completeness of our sample down to $M_B = -20$ through statistical tests. From this sample we create V/V_{\max} diagrams for all morphological types, revealing that we are nearly complete to $10 000 \text{ km s}^{-1}$ for galaxies brighter than $M_B = -20$.

We show fractional histograms in Fig. 4 of the distribution of morphological types, $(B - V)_0$ colours, stellar masses and absolute magnitudes (M_B) for the entire sample. Fig. 5 shows the fraction of all galaxies that are classified into different T-types. From Fig. 5,

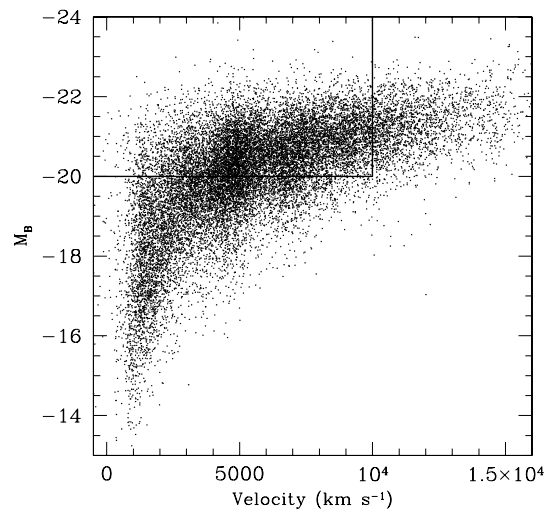


Figure 3. The radial velocity distribution of the galaxies used in our analysis versus their absolute magnitude (M_B). The box formed by the solid line outlines the nearly complete sample we used for analyses that require near complete samples brighter than $M_B < -20$.

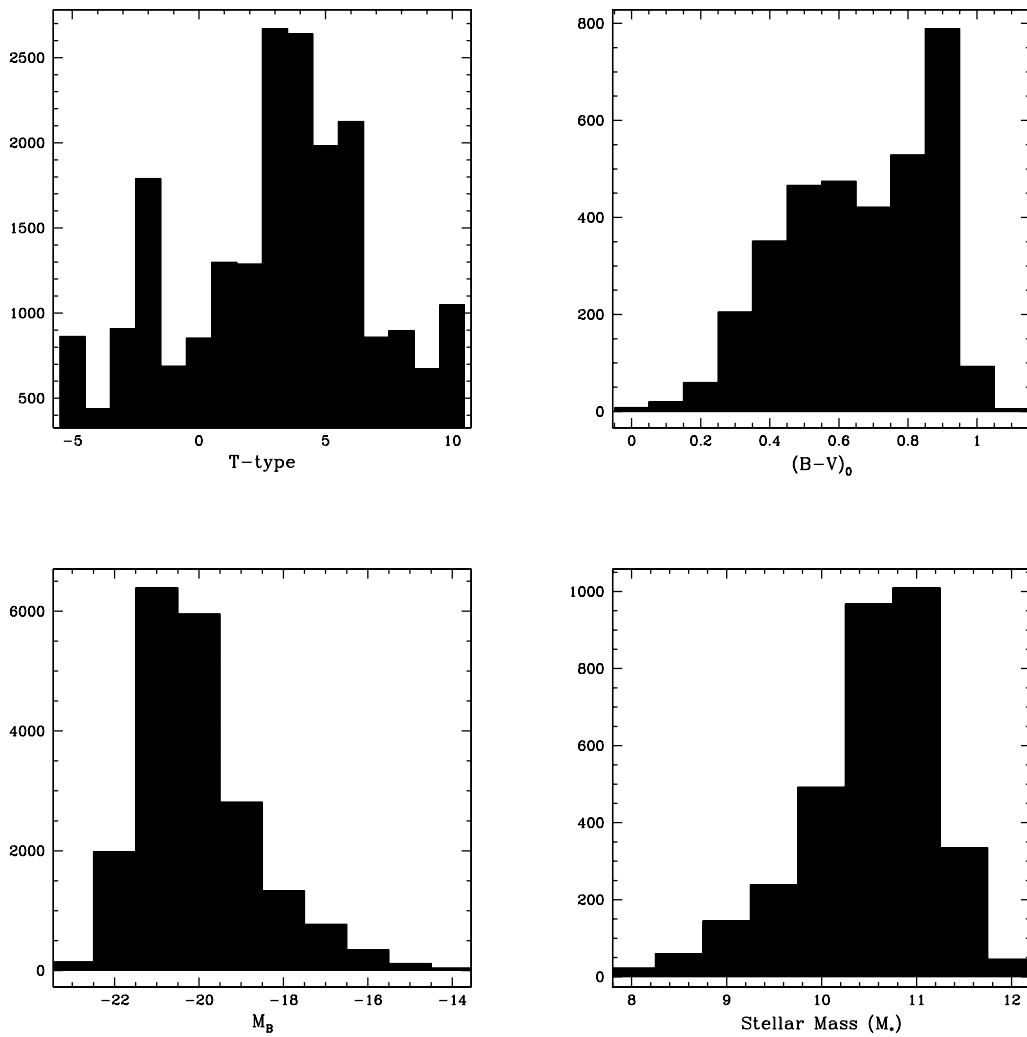


Figure 4. The distribution of morphology (T-type), colour, absolute magnitude and stellar mass (M_*) for all galaxies used in this study. We rapidly become incomplete at $M_B > -20$ and at $M < 5 \times 10^{10} M_\odot$ within our full volume (see Fig. 3). As can be seen, we span the entire range of Hubble types and galaxy colours.

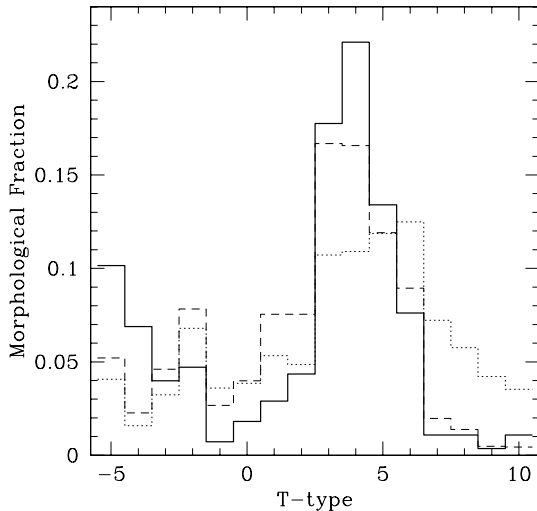


Figure 5. The fraction of different morphological types for all nearby bright galaxies with $M_B < -22$ (solid line), $M_B < -20$ (dashed line) and $M_B < -18$ with $V < 3000 \text{ km s}^{-1}$ (dotted line). The most common galaxy in our sample is therefore a mid-type spiral, which does not change significantly at different luminosity cuts.

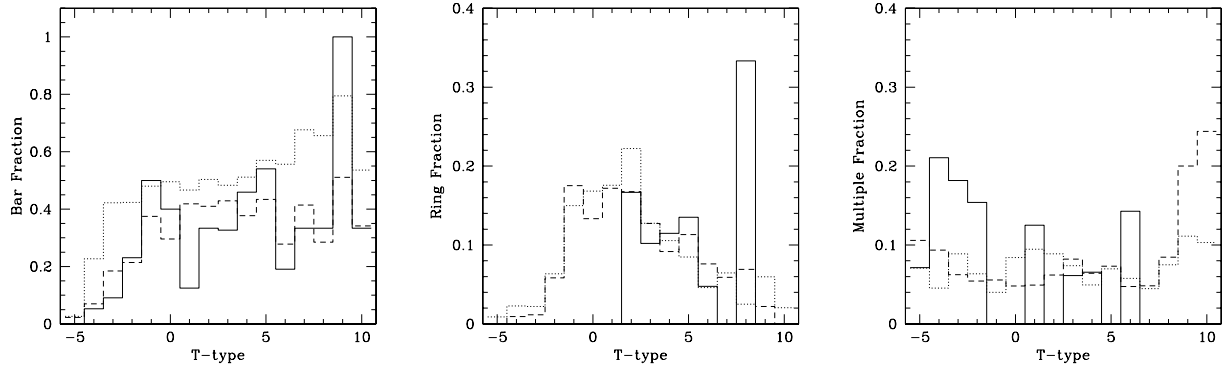
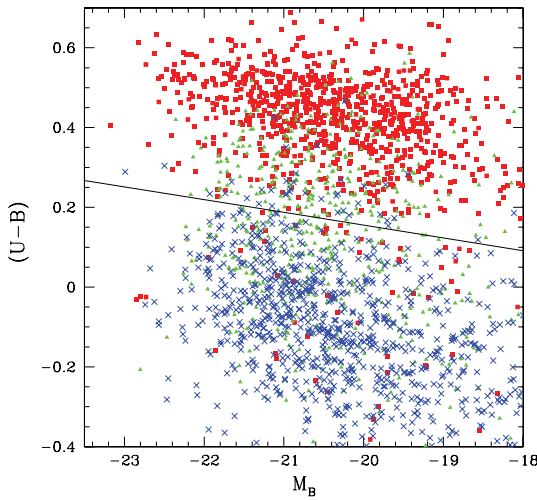
the most common galaxy type in the nearby universe appears to be mid-/late-type spirals, with a peak fraction at T-type = 4 (Sbc). This peak remains unchanged when we cut the sample at brighter, $M_B < -22$, or fainter, $M_B < -18$, limits.

The relative percentages of nearby galaxies with different morphological types are listed in Table 1. It appears that ~ 75 per cent of all nearby bright galaxies with $M_B < -20$ are spirals, with ~ 40 per cent late-type spirals (Sb-Sc). Thus, in the nearby universe most bright galaxies (with $M_B < -20$) are spirals with small bulges. After accounting for spatial incompleteness in the catalogue, we further find that the total number density of spirals is $\sim 3 \times 10^6 \text{ Gpc}^{-3}$ at $M_B < -20$ (Table 1).

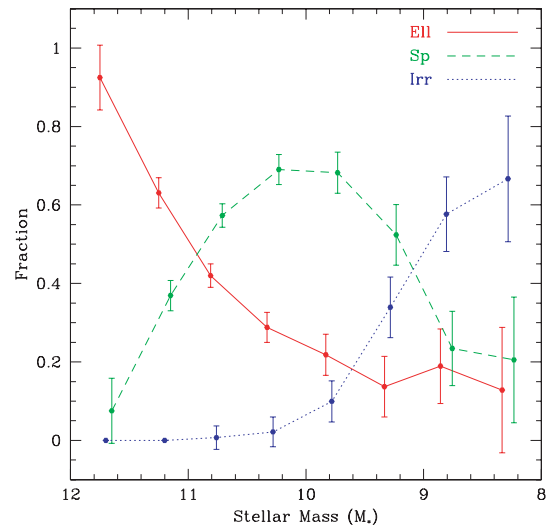
Early-type galaxies, including ellipticals and S0s, account for nearly all of the remainder (22 per cent) of nearby bright galaxies, with the rest ~ 2 per cent irregulars (Table 1). These number densities and morphological type fractions are being directly compared to bright galaxies at high redshifts where these same properties can now be determined (e.g. Conselice 2004; Conselice et al. 2005a). Fig. 6 shows the fraction of each morphological classed type that is also classified as having a bar, ring or part of a multiple system, which we discuss below.

Table 1. Morphological fractions and densities of nearby bright galaxies.

$M_B = -22$	(# Gpc $^{-3} h_{100}^3$)	Fraction	$M_B = -21$	(# Gpc $^{-3} h_{100}^3$)	Fraction	$M_B = -20$	(# Gpc $^{-3} h_{100}^3$)	Fraction
E	$2.0 \pm 0.8 \times 10^4$	0.19	E	$1.3 \pm 0.4 \times 10^5$	0.09	E	$2.7 \pm 0.8 \times 10^5$	0.07
S0	$1.1 \pm 0.5 \times 10^4$	0.10	S0	$1.6 \pm 0.5 \times 10^5$	0.12	S0	$5.7 \pm 1.5 \times 10^5$	0.15
eDisk	$2.5 \pm 1.0 \times 10^4$	0.25	eDisk	$4.8 \pm 1.3 \times 10^5$	0.36	eDisk	$1.3 \pm 0.3 \times 10^6$	0.36
IDisk	$4.5 \pm 1.6 \times 10^4$	0.44	IDisk	$5.4 \pm 1.5 \times 10^5$	0.41	IDisk	$1.5 \pm 0.4 \times 10^6$	0.39
Irr	$2.4 \pm 1.8 \times 10^3$	0.02	Irr	$2.0 \pm 0.8 \times 10^4$	0.02	Irr	$8.4 \pm 2.7 \times 10^4$	0.02

**Figure 6.** The fraction of different galaxy types that have morphological evidence for the presence of bars, rings and multiple components. These fractions are also plotted as a function of luminosity, with $M_B < -22$ (solid line), $M_B < -20$ (long-dashed line) and $M_B < -18$ with $V < 3000 \text{ km s}^{-1}$ (dotted line). As can be seen, the bar fraction is roughly constant at T-types > 0 , while ringed galaxies are typically early-type spirals, and galaxies with a multiple component classification tend to span all Hubble types.**Figure 7.** The colour–magnitude relation for galaxies in our sample. The solid line divides red-sequence galaxies from blue-cloud galaxies (Faber et al. 2005). Early-types are denoted by solid red squares, while later types (T-type > 3) are labelled as blue crosses, and mid-types (T-type > 0 and T-type < 3) are labelled as green triangles.

Another feature we investigate is how galaxy morphology correlates with the positions of galaxies in the colour–magnitude plane (Fig. 7). There is a well-characterized red sequence and blue cloud in the $(U - B)_0$ versus M_B diagram (e.g. Baldry et al. 2004), which has been proposed as a fundamental feature for understanding how galaxies have evolved. When we label the morphological types of galaxies on the colour–magnitude diagram we find a good correlation between the morphologies of galaxies and their positions. The early-types (denoted by solid red squares) are mostly on the red se-

**Figure 8.** The fractional contribution of various morphological types to the local stellar mass density down to a lower limit of $M_* = 10^8 M_\odot$. The solid line shows the ellipticals, the dashed line spirals, and the dotted line irregular galaxies.

quence, while later types (T-type > 3 , blue crosses) are in the blue cloud, and mid-types (T-type > 0 and T-type < 3) are in between.

This is also the case for stellar masses, with the $M_* > 10^{11} M_\odot$ galaxies mostly ellipticals on the red sequence. Lower mass galaxies are increasingly bluer. This can also be seen in Fig. 8, where we plot the morphological fraction as a function of stellar mass. At the highest masses, nearly all galaxies are ellipticals, but this gradually changes, and by $M_* = 10^{11} M_\odot$ ellipticals and spirals each represent about ~ 50 per cent of the population. At the low-mass end, irregulars

Table 2. Bar, ring and multiple component fractions as a function of morphology for galaxies with $M_B < -20$.

Type	Bar (# Gpc $^{-3} h_{100}^3$)	Fraction	Type	Ring (# Gpc $^{-3} h_{100}^3$)	Fraction	Type	Multiple (# Gpc $^{-3} h_{100}^3$)	Fraction
E	$1.2 \pm 0.5 \times 10^4$	0.01	E	$9.6 \pm 10 \times 10^2$	0.00	E	$3.0 \pm 1.1 \times 10^4$	0.11
S0	$1.2 \pm 0.4 \times 10^5$	0.10	S0	$3.6 \pm 1.4 \times 10^4$	0.09	S0	$3.3 \pm 1.3 \times 10^4$	0.13
eDisk	$5.3 \pm 1.4 \times 10^5$	0.44	eDisk	$2.0 \pm 0.6 \times 10^5$	0.52	eDisk	$9.1 \pm 2.9 \times 10^4$	0.35
IDisk	$5.2 \pm 1.4 \times 10^5$	0.43	IDisk	$1.4 \pm 0.4 \times 10^5$	0.37	IDisk	$9.3 \pm 3.0 \times 10^4$	0.36
Irr	$2.3 \pm 0.9 \times 10^4$	0.02	Irr	$4.7 \pm 3.0 \times 10^3$	0.01	Irr	$1.2 \pm 0.6 \times 10^4$	0.05

begin to dominate the population, with spirals accounting for only 20 per cent of the population at $M_* < 10^9 M_\odot$ and ellipticals accounting for about 10 per cent.

4.1.1 Bars

Bars and rings are usually, but not uniquely, associated with spiral galaxies (e.g. Buta & Combes 1996). Bars are dynamical features that reveal, and contribute to, several galaxy evolution processes such as star formation and AGN activity (Barnes & Hernquist 1992), or galaxy interactions. It is debated however whether bars are a fundamental feature of galaxies that should be used in classifications (e.g. Abraham & Merrifield 2000; Conselice 2003). The evolution of bars through cosmic time is also debated, although there are some claims that the bar fraction and sizes of discs have not evolved since $z \sim 1$ (Jogee et al. 2004; Ravindranath et al. 2004). As the evolution of bars will continue to be addressed in the future through observations with the *HST*, we compute basic physical information on barred galaxies in the nearby universe for comparison purposes (Fig. 6a, Table 2).

Table 2 lists, for all barred galaxies in the nearby universe, the fractional breakdown of host galaxy morphological type, and the number densities of each type, for systems brighter than $M_B < -20$. For example, 43 per cent of nearby bright barred galaxies are found in late-type discs, and late-type discs with bars have a total number density of $5.2 \pm 1.4 \times 10^5 h_{100}^3$ galaxies Gpc $^{-3}$. Not surprisingly, we find that almost all (97 per cent) of barred galaxies are classified as discs/S0s, with an equal proportion belonging to early and late-types. Roughly 10 per cent of all barred galaxies are S0s, while 3 per cent of classified barred galaxies are ellipticals and irregular galaxies. The small fraction of bars that are found in ellipticals shows that these systems have been misclassified, as a bar needs a disc to exist.

By examining the fraction of galaxies in each morphological type that are barred (plotted in Fig. 6), we find that roughly 50 per cent of all disc galaxies are barred, while the fraction of barred galaxies increases for later types. There is also a fairly high fraction of nearby galaxies with bars, with a number density in the nearby universe of $\sim 1.2 \times 10^6 h_{100}^3$ barred galaxies Gpc $^{-3}$.

4.1.2 Rings

Rings often follow the presence of bars in galaxies (Buta & Combes 1996), and this can be quantitatively demonstrated as they occupy the same types of galaxies. Of all ringed galaxies brighter than $M_B < -20$, nearly all (98 per cent) are located in discs/S0s (Table 2). The fraction of ringed galaxies which are hosted inside ellipticals, S0s and irregulars is similar to the fraction with bars. There are however fewer ringed galaxies than barred galaxies in the nearby universe, with a number density of 3.8×10^5 ringed galaxies Gpc $^{-3}$. Fig. 6(b)

shows the fraction of galaxies of all morphological types with rings, revealing that early discs are more likely to host a ring than later types.

4.1.3 Multiple components

In addition to bars and rings, the RC3 also includes a classification for galaxies that have multiple components. Intuitively, this might correlate with the presence of merging activity. About 71 per cent of galaxies classified as having multiple components are discs, while 11, 13 and 5 per cent of multiple galaxies are ellipticals, S0s and irregulars, respectively. However, a different pattern emerges when we consider the fractions of each galaxy type that have a multiple classification. Fig. 6(c) plots the fraction of galaxies in each T-type that have morphological evidence for multiple components. This demonstrates that only about 5–10 per cent of all galaxies in the RC3 are classified as multiple galaxies. A higher fraction of irregulars are classified as having multiple components, although this is likely partially due to low number statistics. If these fractions are tracing the merging activity of galaxies in the nearby universe, the derived fraction of 5 per cent is close to the $z \sim 0$ merger fraction estimates from pairs (e.g. Patton et al. 2000).

5 GALAXY PROPERTIES AND THEIR CORRELATIONS

5.1 Statistical analysis of the nearby galaxy population

We now examine how the 14 properties described in Section 3.1 correlate with each other, and how strongly. We do this by performing Spearman rank correlation tests on various cuts of our data (Tables 3–6). These correlation analyses are performed on the entire sample (Table 3), when divided by early and late morphological types (Table 4), colour at $(B - V)_0 = 0.7$ (Table 5), and absolute magnitude at $M_B = -20$ (Table 6). Our sample for the Spearman rank correlations include the RC3 sample out to radial velocities of 15 000 km s $^{-1}$. We discuss in specific cases where not having a volume-limited sample may be affecting our results.

The correlation matrix of our entire sample (Table 3) reveals several strong relationships, including: between V_S and M_B (Faber–Jackson), $\log V_{\max}$ and M_B (Tully–Fisher) and size (R) with M_B (Kormendy relation). However, the relations we find are weaker than these scaling relationships, as the sample here has not been divided into different morphological types. In general however, there are many correlations between the 14 parameters, revealing that to one degree or another most properties of galaxies are interrelated. Is this interrelation the result of a single principle, or a group of physical principles producing different observational effects? For example, it is possible that size and M_B have a strong correlation because they both fundamentally scale with an underlying feature, which is likely the total mass? The same is also true for the strong correlation

Table 3. Spearman correlation matrix for all galaxies.

	T-type	R	$\langle \mu \rangle_e$	$(U - B)_0$	$(B - V)_0$	W_{20}	V_S	H I	FIR	λ	V_{\max}	M_B	I	ρ	M_*
T-type	1.00	-0.24	0.53	-0.79	-0.80	-0.51	-0.43	0.18	0.13	0.91	-0.50	0.25	0.23	-0.14	-0.68
R	-0.24	1.00	0.08	0.23	0.20	0.66	0.48	-0.76	-0.55	-0.62	0.65	-0.85	-0.36	-0.13	0.51
$\langle \mu \rangle_e$	0.53	0.08	1.00	-0.35	-0.36	-0.38	0.09	-0.01	0.08	0.56	-0.35	0.00	0.07	-0.10	-0.07
$(U - B)_0$	-0.79	0.23	-0.35	1.00	0.91	0.51	0.60	0.04	0.03	-0.67	0.48	-0.23	-0.30	0.19	0.75
$(B - V)_0$	-0.80	0.20	-0.36	0.91	1.00	0.47	0.57	0.09	0.03	-0.64	0.47	-0.19	-0.28	0.22	0.80
W_{20}	-0.51	0.66	-0.38	0.51	0.47	1.00	0.30	-0.54	-0.39	-0.72	0.87	-0.68	-0.38	-0.03	0.51
V_S	-0.43	0.48	0.09	0.60	0.57	0.30	1.00	0.09	0.07	-0.31	0.21	-0.55	-0.16	0.06	0.67
H I	0.18	-0.76	-0.01	0.04	0.09	-0.54	0.09	1.00	0.56	0.53	-0.55	0.68	0.23	0.2	-0.05
FIR	0.13	-0.55	0.08	0.03	0.03	-0.39	0.07	0.56	1.00	0.40	-0.46	0.64	0.05	0.23	-0.08
λ	0.91	-0.62	0.56	-0.67	-0.64	-0.72	-0.31	0.53	0.40	1.00	-0.72	0.67	0.40	-0.03	-0.51
V_{\max}	-0.50	0.65	-0.35	0.48	0.47	0.87	0.21	-0.55	-0.46	-0.72	1.00	-0.69	-0.36	-0.05	0.55
M_B	0.25	-0.85	0.00	-0.23	-0.19	-0.68	-0.55	0.68	0.64	0.67	-0.69	1.00	0.31	0.10	-0.59
I	0.23	-0.36	0.07	-0.30	-0.28	-0.38	-0.16	0.23	0.05	0.40	-0.36	0.31	1.00	-0.01	-0.28
ρ	-0.14	-0.13	-0.10	0.19	0.22	-0.03	0.06	0.20	0.23	-0.03	-0.05	0.10	-0.01	1.00	0.13
M_*	-0.68	0.51	-0.07	0.75	0.80	0.51	0.67	-0.05	-0.08	-0.51	0.55	-0.59	-0.28	0.13	1.00

Spearman correlation matrix for all the galaxies in our sample. Displayed are the correlation between various physical properties, including morphology (T-type), radius (R), surface brightness ($\langle \mu \rangle_e$), colour [both $(U - B)_0$ and $(B - V)_0$], H I linewidth (W_{20}), central velocity dispersion (V_S), H I and far-infrared line fluxes (FIR), the luminosity class (λ), the maximum rotation velocity (V_{\max}), the absolute magnitude (M_B), an interaction index (I), local density (ρ) and the stellar mass M_* . The numbers in bold show the strongest correlations between the various parameters. Tables 4–6 show these correlations after the same is divided into early/late, red/blue and bright/faint systems.

between both M_B and size with internal velocities – as things get bigger and brighter they are likely to have more mass, an effect traced by larger internal motions.

We divide these parameters into three classes, following the ideas described in Bershady et al. (2000, hereafter BJC00). BJC00 determined from an analysis of nearby galaxy images that galaxies can be classified according to scale, form and spectral index. In this study colour represents the spectral index, scale includes the size, various fluxes, internal velocities and stellar mass, while form is given by the T-type, bars and the multiple component classification. We investigate which of these measurable properties are the most fundamental, and which are the most useful for classifying galaxies.

5.1.1 Form correlations

We use the T-type to represent the form of a galaxy and to first order assume it correlates with the bulge-to-disc ratio of each galaxy (see also Conselice 2003). T-types (or Hubble types) have been known since at least Holmberg (1958) to correlate broadly with other physical properties, such as recent star formation. Almost by definition this should be the case, as ellipticals and S0s, which populate the earlier T-types, appear fundamentally different from later type galaxies. This difference has been described in more detail by, for example, Roberts & Haynes (1994). It is not yet clear however which physical properties of galaxies correlate strongest with morphology, and if Hubble morphology is enough to describe the most fundamental aspects of galaxies. With our Spearman correlation coefficients, we can begin to address this question.

Table 3 shows the Spearman coefficients for the entire RC3 galaxy sample. If we consider strong correlations those with coefficients $> |0.5|$ (listed in bold) then T-types correlate strongly with both $(B - V)_0$ and $(U - B)_0$ colours, W_{20} , the luminosity index (λ), V_{\max} , μ_m and M_* . This reveals several things about what a T-type is measuring. Since T-types correlate with bulge-to-total (B/T) ratios, then the strong correlation between T-types and colour is not surprising, as it is well known that the relative contributions of bulge and disc light

correlates with old and young stellar populations. The correlation between the stellar masses of galaxies and Hubble T-type (-0.68 coefficient), is stronger than the correlation between T-type and absolute magnitude (0.25), showing that fundamentally the Hubble sequence (or bulge-to-disc ratio) is partially one of stellar mass. There is likewise a strong correlation (coefficient 0.75–0.8) between stellar mass and colour (Table 1), which we discuss in Section 5.1.2.

T-types also correlate strongly with other scale features, as the strong correlations between T-types and V_{\max} , W_{20} , V_S and M_* demonstrates. The absolute magnitude and size of galaxies do not show the same strong correlation, although later type galaxies are smaller and fainter. This weaker correlation between T-type and magnitude/radius might be the result of magnitude/radii being secondary scale features. This is because the measured size of a galaxy is influenced by both the form of a galaxy (i.e. how light is distributed, for example bulge versus disc components) and the intrinsic scale, and magnitude is influenced by scale, and spectral type, as younger, bluer stars will make a galaxy brighter. In this sense these values are not clean measurements of the scale. However, the internal velocities of galaxies and stellar masses are not affected by these secondary effects, and they thus represent more accurately the scale of a galaxy.

Table 4 shows the Spearman correlation matrix between our 14 parameters when the sample has been divided into early ($T < 1$) and late-type ($T > 1$) galaxies. We repeat the Spearman correlation analysis on both early- and late-types, to determine how correlations between T-types and the other parameters are affected by this division. Table 4 shows that for early-types galaxies with $T < 1$ there is very little to no correlation between T-type and other physical parameters, with the exception of perhaps colour. This is such that later type early-types (E6–7, S0) are bluer and have a slightly lower stellar mass.

When we examine correlations between T-types and physical properties for the late-type galaxies (Table 4) many of the correlations seen in Table 3 remain, but with most weaker. The correlation with colour for the late-types declines from ~ -0.8 to -0.61 , as does the correlation with stellar mass. Interestingly, the mild correlation between T-types and surface brightness (μ_e) seems to remain

Table 4. Spearman correlation matrix for early-(late-)type galaxies.

	T-type FIR	R λ	$\langle \mu \rangle_e$ V_{\max}	$(U - B)_0$ M_B	$(B - V)_0$ I	W_{20} ρ	V_S M_*	H_I
T-type	1.00 (1.00) -0.01 (0.21)	-0.09 (-0.38) 0.26 (0.90)	-0.03 (0.51) 0.05 (-0.55)	-0.38 (-0.61) 0.20 (0.41)	-0.42 (-0.63) -0.05 (0.27)	0.09 (-0.56) -0.09 (-0.03)	-0.33 (-0.42) -0.36 (-0.55)	-0.13 (0.29)
R	-0.09 (-0.38) -0.52 (-0.57)	1.00 (1.00) -0.27 (-0.64)	0.41 (-0.09) 0.45 (0.68)	0.29 (0.41) -0.84 (-0.86)	0.24 (0.36) -0.37 (-0.35)	0.46 (0.68) -0.14 (-0.14)	0.59 (0.24) 0.84 (0.81)	-0.54 (-0.78)
$\langle \mu \rangle_e$	-0.03 (0.51) -0.16 (0.17)	0.41 (-0.09) -0.09 (0.57)	1.00 (1.00) 0.15 (-0.40)	0.14 (-0.25) -0.37 (0.22)	0.11 (-0.27) -0.10 (0.11)	0.16 (-0.42) -0.04 (-0.05)	0.21 (-0.14) 0.44 (-0.21)	-0.34 (0.09)
$(U - B)_0$	-0.38 (-0.61) 0.26 (-0.07)	0.29 (0.41) -0.31 (-0.66)	0.14 (-0.25) 0.30 (0.57)	1.00 (1.00) -0.37 (-0.39)	0.73 (0.83) -0.29 (-0.33)	0.37 (0.56) 0.18 (0.19)	0.51 (0.61) 0.55 (0.68)	0.10 (-0.11)
$(B - V)_0$	-0.42 (-0.63) 0.26 (-0.06)	0.24 (0.36) -0.33 (-0.63)	0.11 (-0.27) 0.30 (0.54)	0.73 (0.83) -0.29 (-0.34)	1.00 (1.00) -0.24 (-0.31)	0.32 (0.5) 0.16 (0.18)	0.47 (0.54) 0.54 (0.71)	0.09 (-0.05)
W_{20}	0.09 (-0.56) -0.26 (-0.40)	0.46 (0.68) -0.19 (-0.73)	0.16 (-0.42) 0.89 (0.87)	0.37 (0.56) -0.44 (-0.7)	0.32 (0.50) -0.28 (-0.39)	1.00 (1.00) -0.04 (-0.03)	0.29 (0.45) 0.41 (0.69)	-0.43 (-0.56)
V_S	-0.33 (-0.42) 0.01 (-0.08)	0.59 (0.24) -0.53 (-0.34)	0.21 (-0.14) 0.2 (0.46)	0.51 (0.61) -0.68 (-0.26)	0.47 (0.54) -0.22 (-0.18)	0.29 (0.45) 0.01 (-0.03)	1.00 (1.00) 0.74 (0.55)	-0.09 (-0.03)
H_I	-0.13 (0.29) 0.63 (0.56)	-0.54 (-0.78) 0.27 (0.56)	-0.34 (0.09) -0.43 (-0.58)	0.1 (-0.11) 0.51 (0.70)	0.09 (-0.05) 0.2 (0.23)	-0.43 (-0.56) 0.21 (0.20)	-0.09 (-0.03) -0.27 (-0.54)	1.00 (1.00)
FIR	-0.01 (0.21) 1.00 (1.00)	-0.52 (-0.57) 0.02 (0.42)	-0.16 (0.17) -0.34 (-0.47)	0.26 (-0.07) 0.58 (0.67)	0.26 (-0.06) 0.12 (0.05)	-0.26 (-0.40) 0.32 (0.21)	0.01 (-0.08) -0.24 (-0.54)	0.63 (0.56)
λ	0.26 (0.90) 0.02 (0.42)	-0.27 (-0.64) 1.00 (1.00)	-0.09 (0.57) -0.18 (-0.73)	-0.31 (-0.66) 0.32 (0.69)	-0.33 (-0.63) 0.02 (0.41)	-0.19 (-0.73) -0.28 (-0.02)	-0.53 (-0.34) -0.48 (-0.73)	0.27 (0.56)
V_{\max}	0.05 (-0.55) -0.34 (-0.47)	0.45 (0.68) -0.18 (-0.73)	0.15 (-0.40) 1.00 (1.00)	0.3 (0.57) -0.48 (-0.72)	0.30 (0.54) -0.32 (-0.37)	0.89 (0.87) -0.09 (-0.05)	0.20 (0.46) 0.39 (0.74)	-0.43 (-0.58)
M_B	0.20 (0.41) 0.58 (0.67)	-0.84 (-0.86) 0.32 (0.69)	-0.37 (0.22) -0.48 (-0.72)	-0.37 (-0.39) 1.00 (1.00)	-0.29 (-0.34) 0.30 (0.31)	-0.44 (-0.70) 0.05 (0.12)	-0.68 (-0.26) -0.94 (-0.88)	0.51 (0.70)
I	-0.05 (0.27) 0.12 (0.05)	-0.37 (-0.35) 0.02 (0.41)	-0.1 (0.11) -0.32 (-0.37)	-0.29 (-0.33) 0.30 (0.31)	-0.24 (-0.31) 1.00 (1.00)	-0.28 (-0.39) 0.00 (-0.01)	-0.22 (-0.18) -0.22 (-0.35)	0.20 (0.23)
ρ	-0.09 (-0.03) 0.32 (0.21)	-0.14 (-0.14) -0.28 (-0.02)	-0.04 (-0.05) -0.09 (-0.05)	0.18 (0.19) 0.05 (0.12)	0.16 (0.18) 0.00 (-0.01)	-0.04 (-0.03) 1.00 (1.00)	0.01 (-0.03) 0.08 (0.10)	0.21 (0.20)
M_*	-0.36 (-0.55) -0.24 (-0.54)	0.84 (0.81) -0.48 (-0.73)	0.44 (-0.21) 0.39 (0.74)	0.55 (0.68) -0.94 (-0.88)	0.54 (0.71) -0.22 (-0.35)	0.41 (0.69) 0.08 (0.10)	0.74 (0.55) 1.00 (1.00)	-0.27 (-0.54)

for the late-types, such that later types have a lower surface brightness. This is perhaps the only correlation in the Hubble sequence (besides V_{\max}) which is driven mostly by later type galaxies alone.

Most correlations between physical features and Hubble types is strongest when considering the entire sequence. One exception to this is the correlation between stellar mass and colour which remains strong after dividing the sample into early/late Hubble types (Table 4). This shows that this correlation is not driven entirely by morphology. There is however little correlation within the early-types themselves, with the exception of scale-scale correlations. This demonstrates that the division of early-types on to the Hubble sequence, which is typically done by estimating the axis ratios of galaxies (Sandage 1961), is largely devoid of much useful physical information (Kormendy & Bender 1996). The fact that T-types correlate strongly with colour and stellar mass can be understood to first order if star formation follows the presence of discs. Galaxies with types $T > 1$ have a diversity in B/T ratios, and a mix of segregated stellar populations (Papovich et al. 2003), while ellipticals have B/T ~ 1 and tend to have nearly homogenous old stellar populations.

5.1.2 Spectral type correlations

As discussed in Section 5.1.1 galaxy T-types correlate strongly with colour. Spectral type, as denoted by either the $(B - V)_0$ or $(U - B)_0$ colour, also correlates well with the internal velocities of galaxies, that is, W_{20} , V_{\max} and V_S as well as stellar masses (Table 3). The colours of galaxies however do not strongly correlate with any other galaxy property, including sizes, H_I /FIR luminosities and absolute magnitude.

Late-types are blue, and systems with lower internal velocities, and lower stellar masses are also bluer, as discussed above. There is no a priori reason for galaxies with lower internal velocities, lower stellar masses, to have average younger stellar populations, while more massive systems have a larger fraction of older stars. This correlation between ongoing star formation, as revealed through bluer colours, and stellar mass is a form of the downsizing seen up to $z \sim 1$ (Bundy et al. 2005, 2006), which is still an unexplained physical effect that dominates the way galaxies formed.

We separated the RC3 sample into red and blue systems, divided at $(B - V)_0 = 0.7$, and then redetermine how these various correlations change (Table 5). We find a similar effect as when we divide

Table 5. Spearman correlation matrix for red/(blue) galaxies divided at $(B - V)_0 = 0.7$.

	T-type FIR	R λ	$\langle \mu \rangle_e$ V_{\max}	$(U - B)_0$ M_B	$(B - V)_0$ I	W_{20} ρ	V_S M_*	H_I
T-type	1.00 (1.00) -0.24 (0.23)	0.02 (-0.20) 0.72 (0.88)	0.07 (0.54) 0.16 (-0.45)	-0.58 (-0.43) 0.07 (0.28)	-0.55 (-0.48) -0.01 (0.21)	0.09 (-0.48) 0.00 (0.00)	-0.38 (-0.27) -0.23 (-0.39)	-0.41 (0.19)
R	0.02 (-0.20) -0.49 (-0.55)	1.00 (1.00) 0.00 (-0.60)	0.48 (0.02) 0.40 (0.62)	0.06 (0.39) -0.88 (-0.87)	0.03 (0.34) -0.11 (-0.36)	0.36 (0.61) -0.04 (0.01)	0.56 (0.40) 0.83 (0.84)	-0.63 (-0.81)
$\langle \mu \rangle_e$	0.07 (0.54) -0.22 (0.21)	0.48 (0.02) 0.23 (0.46)	1.00 (1.00) 0.09 (-0.28)	-0.08 (-0.14) -0.43 (0.13)	-0.05 (-0.20) -0.01 (0.04)	-0.04 (-0.36) -0.08 (-0.02)	0.18 (0.10) 0.38 (-0.16)	-0.40 (0.01)
$(U - B)_0$	-0.58 (-0.43) 0.39 (-0.19)	0.06 (0.39) -0.39 (-0.60)	-0.08 (-0.14) -0.04 (0.49)	1.00 1.00 -0.14 (-0.37)	0.70 (0.75) -0.02 (-0.31)	0.03 (0.48) 0.06 (0.09)	0.52 (0.35) 0.32 (0.57)	0.28 (-0.22)
$(B - V)_0$	-0.55 (-0.48) 0.35 (-0.16)	0.03 (0.34) -0.24 (-0.59)	-0.05 (-0.20) -0.05 (0.48)	0.70 (0.75) -0.08 (-0.33)	1.00 (1.00) 0.06 (-0.28)	0.00 (0.44) 0.08 (0.08)	0.48 (0.20) 0.35 (0.62)	0.27 (-0.16)
W_{20}	0.09 (-0.48) -0.20 (-0.41)	0.36 (0.61) -0.05 (-0.66)	-0.04 (-0.36) 0.8 (0.85)	0.03 (0.48) -0.34 (-0.66)	0.00 (0.44) -0.21 (-0.43)	1.00 (1.00) 0.00 (0.05)	0.25 (0.32) 0.34 (0.69)	-0.32 (-0.55)
V_S	-0.38 (-0.27) 0.11 (-0.38)	0.56 (0.40) -0.20 (-0.36)	0.18 (0.10) 0.20 (0.36)	0.52 (0.35) -0.66 (-0.39)	0.48 (0.20) 0.00 (-0.24)	0.25 (0.32) 0.08 (-0.17)	1.00 (1.00) 0.72 (0.46)	-0.03 (-0.30)
H_I	-0.41 (0.19) 0.57 (0.53)	-0.63 (-0.81) -0.05 (0.52)	-0.4 (0.01) -0.41 (-0.58)	0.28 (-0.22) 0.58 (0.78)	0.27 (-0.16) 0.04 (0.25)	-0.32 (-0.55) 0.09 (0.10)	-0.03 (-0.3) -0.50 (-0.68)	1.00 (1.00)
FIR	-0.24 (0.23) 1.00 (1.00)	-0.49 (-0.55) -0.06 (0.45)	-0.22 (0.21) -0.30 (-0.50)	0.39 (-0.19) 0.52 (0.73)	0.35 (-0.16) 0.01 (0.03)	-0.20 (-0.41) 0.03 (0.13)	0.11 (-0.38) -0.43 (-0.66)	0.57 (0.53)
λ	0.72 (0.88) -0.06 (0.45)	0.00 (-0.60) 1.00 (1.00)	0.23 (0.46) -0.09 (-0.67)	-0.39 (-0.60) -0.01 (0.67)	-0.24 (-0.59) 0.10 (0.37)	-0.05 (-0.66) -0.09 (0.00)	-0.2 (-0.36) -0.02 (-0.73)	-0.05 (0.52)
V_{\max}	0.16 (-0.45) -0.30 (-0.50)	0.40 (0.62) -0.09 (-0.67)	0.09 (-0.28) 1.00 (1.00)	-0.04 (0.49) -0.44 (-0.70)	-0.05 (0.48) -0.20 (-0.40)	0.80 (0.85) -0.09 (0.01)	0.20 (0.36) 0.43 (0.74)	-0.41 (-0.58)
M_B	0.07 (0.28) 0.52 (0.73)	-0.88 (-0.87) -0.01 (0.67)	-0.43 (0.13) -0.44 (-0.70)	-0.14 (-0.37) 1.00 (1.00)	-0.08 (-0.33) 0.11 (0.32)	-0.34 (-0.66) 0.01 (0.04)	-0.66 (-0.39) -0.95 (-0.93)	0.58 (0.78)
I	-0.01 (0.21) 0.01 (0.03)	-0.11 (-0.36) 0.10 (0.37)	-0.01 (0.04) -0.20 (-0.40)	-0.02 (-0.31) 0.11 (0.32)	0.06 (-0.28) 1.00 (1.00)	-0.21 (-0.43) -0.02 (-0.03)	0.00 (-0.24) -0.07 (-0.35)	0.04 (0.25)
ρ	0.00 (0.00) 0.03 (0.13)	-0.04 (0.01) -0.09 (0.00)	-0.08 (-0.02) -0.09 (0.01)	0.06 (0.09) 0.01 (0.04)	0.08 (0.08) -0.02 (-0.03)	0.00 (0.05) 1.00 (1.00)	0.08 (-0.17) 0.02 (0.01)	0.09 (0.10)
M_*	-0.23 (-0.39) -0.43 (-0.66)	0.83 (0.84) -0.02 (-0.73)	0.38 (-0.16) 0.43 (-0.74)	0.32 (0.57) -0.95 (-0.93)	0.35 (0.62) -0.07 (-0.35)	0.34 (0.69) 0.02 (0.01)	0.72 (0.46) 1.00 (1.00)	-0.50 (-0.68)

the sample by morphology. Red galaxies show fewer correlations between different parameters (Table 5), again with the exception of colour, such that later types with red colours, are bluer. However, as for early-types, there is little correlation between colour and stellar mass for red galaxies. Star-forming blue galaxies have physical properties that correlate well with each other, that is, stellar mass with colour, H_I with stellar mass, and size with V_{\max} . Interestingly, the correlation between T-types and colour within the red galaxies is slightly stronger than it is for the blue galaxies (~ -0.55 versus -0.45). There is still a fairly strong (~ 0.5) correlation between $(B - V)_0$ colour with internal velocity dispersion (V_S), and size with V_S (0.56), for red galaxies, revealing that these relationships are independent of star formation.

5.1.3 Scale

As was mentioned earlier, the different scale features of galaxies, namely, size, stellar mass, internal velocities, magnitude, H_I and FIR magnitudes, all correlate with each other with coefficients ~ 0.5 –0.7 for most correlations. Some of these strong correlations are: R with W_{20} (0.66), V_S (0.48), V_{\max} (0.65), M_B (−0.85) and M_* (0.51); and

M_B with W_{20} (−0.68), V_S (−0.55) and V_{\max} (−0.69). This indicates that measures of scale correlate with each other, and are independent of classification. There is also a correlation between scale parameters, particularly internal velocities, and the morphological T-type, as discussed in Section 5.1.1.

Correlations between scale parameters remain when examining galaxies divided by morphology, colour and absolute magnitude (Tables 4–6). For example, the correlation between M_B and R remains quite strong no matter how the sample is divided with coefficients of ~ 0.85 . Other strong correlations are between internal velocities, (V_S), for early-types, (V_{\max}) for late-types and absolute magnitude (M_B), with values −0.68, −0.72, respectively.

Correlations for systems divided into blue and red galaxies at $(B - V) = 0.7$, and for systems divided into ‘bright’ galaxies with $M_B > -20$, and faint galaxies with $M_B < -20$ show a similar dichotomy as late-/early-types (Tables 5–6). Likewise, as for red galaxies and early-types, the bright systems tend to have weaker correlations compared to when the entire magnitude range is considered.

For the more luminous galaxies, parameters that correlate strongly are: magnitude/stellar mass with size scalings and

Table 6. Spearman correlation matrix for bright/(faint) galaxies divided at $M_B = -20$.

	T-type FIR	R λ	$\langle \mu \rangle_e$ V_{\max}	$(U - B)_0$ M_B	$(B - V)_0$ I	W_{20} ρ	V_S M_*	H_I
T-type	1.00 (1.00) 0.11 (0.31)	-0.08 (-0.16) 0.67 (0.95)	0.38 (0.68) -0.29 (-0.51)	-0.80 (-0.75) 0.02 (0.38)	-0.81 (-0.76) 0.06 (0.21)	-0.24 (-0.51) -0.14 (-)	-0.52 (-0.19) -0.65 (-0.64)	-0.17 (0.10)
R	-0.08 (-0.16) -0.29 (-0.42)	1.00 (1.00) -0.24 (-0.41)	0.28 (-0.04) 0.41 (0.50)	0.15 (0.16) -0.66 (-0.73)	0.13 (0.13) -0.20 (-0.31)	0.44 (0.49) -0.13 (-)	0.29 (0.24) 0.54 (0.52)	-0.52 (-0.71)
$\langle \mu \rangle_e$	0.38 (0.68) 0.22 (0.22)	0.28 (-0.04) 0.28 (0.63)	1.00 (1.00) -0.17 (-0.46)	-0.17 (-0.54) -0.20 (0.32)	-0.21 (-0.55) -0.04 (0.06)	-0.17 (-0.49) -0.10 (-)	0.11 (-0.31) 0.00 (-0.51)	-0.28 (-0.08)
$(U - B)_0$	-0.8 (-0.75) 0.3 (-0.16)	0.15 (0.16) -0.55 (-0.6)	-0.17 (-0.54) 0.37 (0.52)	1.00 (1.00) -0.07 (-0.31)	0.91 (0.90) -0.21 (-0.23)	0.4 (0.47) 0.19 (-)	0.65 (0.54) 0.74 (0.78)	0.27 (0.19)
$(B - V)_0$	-0.81 (-0.76) 0.23 (-0.17)	0.13 (0.13) -0.48 (-0.59)	-0.21 (-0.55) 0.38 (0.49)	0.91 (0.90) -0.06 (-0.28)	1.00 (1.00) -0.21 (-0.16)	0.36 (0.44) 0.22 (-)	0.61 (0.53) 0.80 (0.81)	0.29 (0.25)
W_{20}	-0.24 (-0.51) -0.12 (-0.39)	0.44 (0.49) -0.35 (-0.62)	-0.17 (-0.49) 0.78 (0.82)	0.40 (0.47) -0.39 (-0.59)	0.36 (0.44) -0.22 (-0.34)	1.00 (1.00) -0.03 (-)	0.23 (0.34) 0.47 (0.67)	-0.23 (-0.39)
V_S	-0.52 (-0.19) 0.21 (0.14)	0.29 (0.24) -0.34 (-0.32)	0.11 (-0.31) 0.18 (0.16)	0.65 (0.54) -0.34 (-0.38)	0.61 (0.53) -0.13 (-0.19)	0.23 (0.34) 0.05 (-)	1.00 (1.00) 0.66 (0.57)	0.25 (0.10)
H_I	-0.17 (0.10) 0.32 (0.42)	-0.52 (-0.71) 0.07 (0.26)	-0.28 (-0.08) -0.25 (-0.43)	0.27 (0.19) 0.39 (0.55)	0.29 (0.25) -0.02 (0.20)	-0.23 (-0.39) 0.21 (-)	0.25 (0.10) -0.08 (-0.14)	1.00 (1.00)
FIR	0.11 (0.31) 1.00 (1.00)	-0.29 (-0.42) 0.20 (0.44)	0.22 (0.22) -0.24 (-0.45)	0.30 (-0.16) 0.43 (0.54)	0.23 (-0.17) -0.11 (0.05)	-0.12 (-0.39) 0.22 (-)	0.21 (0.14) -0.12 (-0.12)	0.32 (0.42)
λ	0.67 (0.95) 0.20 (0.44)	-0.24 (-0.41) 1.00 (1.00)	0.28 (0.63) -0.37 (-0.64)	-0.55 (-0.60) 0.26 (0.63)	-0.48 (-0.59) 0.13 (0.32)	-0.35 (-0.62) -0.02 (-)	-0.34 (-0.32) -0.46 (-0.78)	0.07 (0.26)
V_{\max}	-0.29 (-0.51) -0.24 (-0.45)	0.41 (0.50) -0.37 (-0.64)	-0.17 (-0.46) 1.00 (1.00)	0.37 (0.52) -0.42 (-0.60)	0.38 (0.49) -0.21 (-0.32)	0.78 (0.82) -0.05 (-)	0.18 (0.16) 0.52 (0.67)	-0.25 (-0.43)
M_B	0.02 (0.38) 0.43 (0.54)	-0.66 (-0.73) 0.26 (0.63)	-0.20 (0.32) -0.42 (-0.60)	-0.07 (-0.31) 1.00 (1.00)	-0.06 (-0.28) 0.11 (0.28)	-0.39 (-0.59) 0.10 (-)	-0.34 (-0.38) -0.61 (-0.75)	0.39 (0.55)
I	0.06 (0.21) -0.11 (0.05)	-0.20 (-0.31) 0.13 (0.32)	-0.04 (0.06) -0.21 (-0.32)	-0.21 (-0.23) 0.11 (0.28)	-0.21 (-0.16) 1.00 (1.00)	-0.22 (-0.34) -0.01 (-)	-0.13 (-0.19) -0.25 (-0.28)	-0.02 (0.20)
ρ	-0.14 (-) 0.22 (-)	-0.13 (-) -0.02 (-)	-0.10 (-) -0.05 (-)	0.19 (-) 0.10 (-)	0.22 (-) -0.01 (-)	-0.03 (-) 1.00 (-)	0.05 (-) 0.15 (-)	0.21 (-)
M_*	-0.65 (-0.64) -0.12 (-0.12)	0.54 (0.52) -0.46 (-0.78)	0.00 (-0.51) 0.52 (0.67)	0.74 (0.78) -0.61 (-0.75)	0.80 (0.81) -0.25 (-0.28)	0.47 (0.67) 0.15 (-)	0.66 (0.57) 1.00 (1.00)	-0.08 (-0.14)

internal velocity (V_S), as well as M_* , colour and T-type among each other (Table 6). This is also the case for fainter galaxies where there is a strong correlation (~ 0.8) between M_* and colour, such that more massive galaxies are redder. Both W_{20} and V_{\max} correlate well with most parameters except with the I index, an indication that for fainter systems V_{\max} is measuring something fundamental about the scale of these systems. This is also true when examining the correlation of internal velocities (V_S) of the more massive systems.

5.1.4 Local density

The local density (hereafter environment) of a galaxy has been known since Hubble (1926) to correlate with galaxy populations. This morphology-density relation can be summarized by stating that in locally dense environments a large fraction of galaxies are early-types (either S0s or ellipticals), while in lower density environments spiral galaxies are more common (e.g. Dressler 1980; Postman & Geller 1984).

We can re-examine the correlation of environment with other physical properties by using the calculated galaxy number density

(ρ) parameter (Section 3.1). We however do not find a strong correlation between ρ and other parameters, including morphological type. This is perhaps because galaxies of all types are found in all environments, but their relative proportions can change, creating, for example, the morphology-density relation. Table 3 shows that the correlations between local density and properties such as colour and T-type have the general trend expected, such as later types and bluer galaxies are found in lower density environments. However, these correlations are not as strong as many others.

5.1.5 Summary of correlations

It is clear from the above discussion that there are strong correlations between various galaxies properties. A few of these correlations, such as size and brightness are very strong, and are independent of other properties such as recent star formation. Perhaps the most interesting correlation is the one between T-type, stellar mass and colour, which all seem to relate to each other.

Scale features, such as size and stellar mass, correlate strongly, which does not change after dividing the population into early/late,

red/blue or bright/faint systems. However, other correlations break down when we examine them within these subsets, showing the scale is a fundamental feature of galaxies.

In particular, many correlations remain for late-type, or star-forming galaxies, as defined by $(B - V) < 0.7$, but do not appear as strong as for the early/red galaxies. These correlations, which break down in the absence of recent star formation are: stellar mass/magnitude with colour and H_I/FIR magnitudes, and T-type with surface brightness. There is also little correlation between T-types and size when galaxies are broken into red/blue systems.

Ongoing star formation is therefore a critical component for trying to understand the properties of galaxies. Finally, if we accept the idea that the strongest correlations with Hubble type reveal its underlying meaning, then the fact that T-types correlate with colour and internal velocities demonstrates that the Hubble sequence is fundamentally one of decreased total mass and increased dominance of young stars, which accounts for its success in the nearby universe.

Note, that the form index, I , which has been shown to correlate with dynamical disturbances (Conselice et al. 2000b), does not correlate strongly with any of the other observational properties we study in this paper (Table 3). This reveals that I is not directly related to, or always causes, other parameters to change, with the exception of perhaps the luminosity index.

5.2 Principal-component analysis

We carry out a principal-component analysis (PCA) of the properties of our sample to determine the most fundamental features needed to describe nearby galaxies. The question we address is whether we can use only morphological type to describe a galaxy's major properties. We perform several PCAs to determine which features cannot be accounted for by other properties, and to reduce the dimensionality of our data set with its 14 parameters.

PCA methods are commonly used in astronomy, and good introductions to the topic can be found in, for example, Faber (1973), Whitmore (1984), Han (1995), Brotherton (1996) and Madgwick et al. (2003). The basic goal of a PCA is to reduce the number of variables (n) to a set of $m < n$ parameter combinations. This is done through the calculation of eigenvectors and eigenvalues for the different parameter combinations. The first eigenvector is a line through the cloud of n data points which minimizes the variance. Remaining eigenvectors are calculated until all the variance is explained. Eigenvalues reveal how much of the variation is accounted for by each eigenvector. Typically the eigenvalue for an eigenvector

must be ≥ 1 to be significant. Before we carry out our various PCAs, we linearize all variables, subtract the mean from each variable, and normalize by the standard deviation.

We performed a large number of PCAs on our data. A typical analysis that includes most of our properties is shown in Table 7. We have created a new index here called 'Vel' which is the internal velocity of our galaxies, V_{\max} , or V_S when V_{\max} is not available. When we calculate the total masses of our galaxies using $\sim R \times V_{\max}^2$, or total masses derived based on scalings derived from models (Conselice et al. 2005b), we find the same correlations. The eigenvectors listed in Table 7 show that several vectors are needed to reach a reasonable accounting of the total variance in galaxy properties. The total summation of the five eigenvectors listed in Table 7 represent 83 per cent of the variance in the properties of galaxies. Due to the errors on the measurements, this is likely the limit for meaningful eigenvectors. In fact, when we plot the eigenvalues for the analysis in Table 7 versus principal-component rank we find a shallow slope past EV 5 than before it, suggesting that these higher components are dominated by noise.

The first eigenvector (EV 1; Table 7) is dominated by M_B , M_* , size (R) and H_I content, which all positively correlate (M_B was converted into a positive linear flux for this analysis). The first vector can therefore be thought of as the scale of the system. The second vector is dominated by the T-type, the $(B - V)_0$ colour, and surface brightness. The strong correlation between Hubble types and colour suggests that this vector measures the presence of recent star formation in a galaxy. Vectors 3 and 4 are both dominated by the merger parameter (I) and the FIR luminosity, and as such it represents the merging properties of galaxies. Vector 5 is dominated by the internal velocities of galaxies.

We find a similar pattern after we remove various variables from the PCA. If we do not consider FIR or surface brightness in the analysis, we find that the eigenvectors are always dominated by I , $(B - V)_0$ and M_* in the first three principal components. We find in general that the T-type is a significant contributor to many components after the analysis is carried out through different cuts in the data.

When we do a basic PCA on our sample separated into only T-types, a spectral index [$(B - V)_0$ colour], the merger index (I) and stellar mass (M_*) we obtain Table 8. We find that the T-type, stellar mass and colour are highly correlated and dominate the first component. The I merger index defines the second principal component, while the third component is dominated by the T-type, and the stellar mass. This shows that the T-type is successful as a general galaxy

Table 7. Principal-component analysis eigenvector projections on to galaxy properties.

Property	EV 1	EV 2	EV 3	EV 4	EV 5
T-type	-0.06	0.61	0.03	-0.07	0.12
R	0.49	0.07	0.08	0.11	-0.07
$\langle \mu \rangle_e$	0.10	0.42	0.36	0.35	0.03
$(B - V)_0$	0.19	-0.55	0.15	0.14	-0.10
Vel	0.19	-0.12	0.07	-0.34	0.90
H _I	0.42	0.28	-0.12	-0.06	-0.06
FIR	0.14	0.06	-0.69	-0.41	-0.19
M_B	0.50	0.09	-0.06	0.02	-0.04
I	-0.06	-0.02	-0.58	0.74	0.34
M_*	0.47	-0.20	0.05	0.11	-0.05
Eigenvalues	3.4 33.6 per cent	2.0 19.7 per cent	1.1 11.1 per cent	0.94 9.4 per cent	0.90 9.0 per cent

Table 8. Eigenvectors for principal-component analysis with T-type, colour and M_* .

Property	EV 1	EV 2	EV 3
T-type	-0.57	-0.13	0.60
$(B - V)_0$	0.63	-0.04	-0.10
I	0.06	0.96	0.23
M_*	0.52	-0.20	0.76
Eigenvalues	2.0	1.02	0.64
	50.8 per cent	25.4 per cent	16.1 per cent

classification criteria as it correlates strongly with colour and stellar mass, and several other properties (cf. Table 3). Therefore the three most fundamental properties for describing nearby galaxies appear to be their scale, recent star formation and the presence of mergers.

From Section 5.1 and Table 3 we know that the interaction/merger index, I , does not correlate strongly with any other galaxy property, with the exception of the luminosity index. The meaning of this is that galaxies which are undergoing a merger cannot be accounted for by other measurable features. When we analyse only galaxies undergoing mergers, defined as objects with $I > 1.5$, we find that three principal components are necessary to describe these systems. In fact, for systems with $M > 1.5$ the correlation between T-type and $(B - V)_0$ colours breaks down. We conclude from the above analyses that our hypothesis, described in Conselice (2003) that mass, star formation and the presence of mergers are fundamental criteria, is a reasonable assumption.

5.3 Galaxies in PCA space

In this section we examine whether the principal-component projections for our sample are correlated, and if different galaxy types separate cleanly within PCA space (see Madgwick et al. 2003, for examples of this using galaxy spectra). For this analysis we examine the principal components shown in Table 8. Fig. 9 shows the correlation between the projections of our galaxies on to their first three eigenvectors listed in Table 8, which as we have discussed, generally correlate with colour (p_1), interactions/mergers (p_2) and stellar mass (p_3). We furthermore label the morphological type of

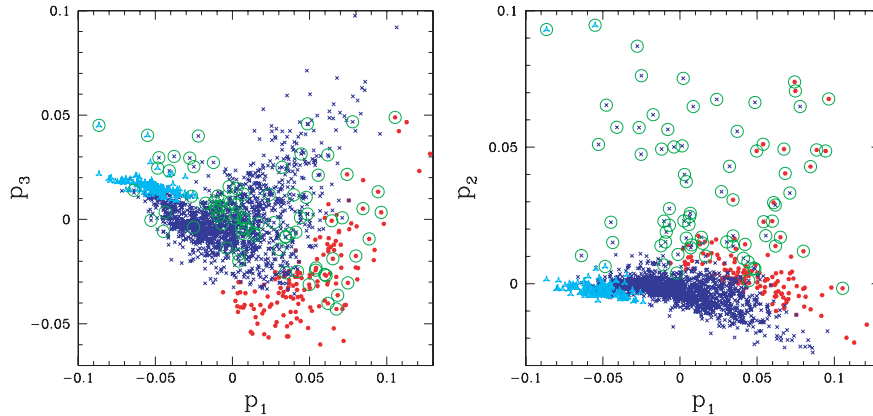


Figure 9. The relation between the projection of galaxies on to the eigenvectors listed in Table 8. The morphological and dynamical state of each galaxy is also noted. The red solid points are the ellipticals and S0s, the blue crosses are the discs, and the cyan triangles are irregulars. The objects circled and in green are those with an interaction/merger index $I > 2$. The three projected components, in which normal galaxies of different types, as well as interacting/merging galaxies, are well separated, trace the scale (p_3), star formation (p_1), and interacting/merging properties (p_2) of galaxies (Section 5.2).

galaxies in Fig. 9, which shows that this relatively simple PCA separates nicely the major galaxy classes: early-types, discs, irregulars and merging galaxies. The left-hand panel of Fig. 9 shows a correlation between the projection of the eigenvectors dominated by recent star formation (colour) and scale (stellar mass). There is however a perpendicular relation as well which is occupied mostly by disc galaxies.

The correlation between p_1 and p_2 shows a similar pattern, but with only a slight correlation between the two eigenvector projections. However, it is clear that interacting and merging galaxies, with $I > 2$, deviate from the nominal relation. Examples of these high- I systems are shown in Fig. 2. There is also a correlation between the second and third eigenvector projections for most galaxies in our sample. Just as in the right-hand panel of Fig. 9, galaxies with a high- I index deviate from this relation with a larger projection on to the second eigenvector.

5.4 The strongest correlations

With our current data set we can address which scaling relations are statistical the strongest for nearby galaxies. While most of these relations are well known and characterized, we discuss several below which are found independent of sample selection. These correlations are: T-type with $(B - V)_0$ colours, T-type with $\log V_{\max}$, radius with absolute magnitude, radius with V_{\max} , $(B - V)_0$ with $\log V_{\max}$, and absolute magnitude with $\log V_{\max}$. The relationship between these parameters are shown in Fig. 10. The best fits between these parameters are

$$T = 0.66 \pm 0.02 \times (B - V)^{-0.15 \pm 0.02},$$

$$T = 2.30 \pm 0.01 \times (\log V_{\max})^{-0.06 \pm 0.003},$$

$$M_B = -15.5 \pm 0.02 \times R^{0.1 \pm 0.004},$$

$$\log V_{\max} = 1.57 \pm 0.001 \times R^{0.12 \pm 0.01},$$

$$\log V_{\max} = 2.64 \pm 0.03 \times (B - V)_0^{0.16 \pm 0.01},$$

$$M_B = -4.7 \pm 0.1 \times \log V_{\max} - 9.8 \pm 0.2.$$

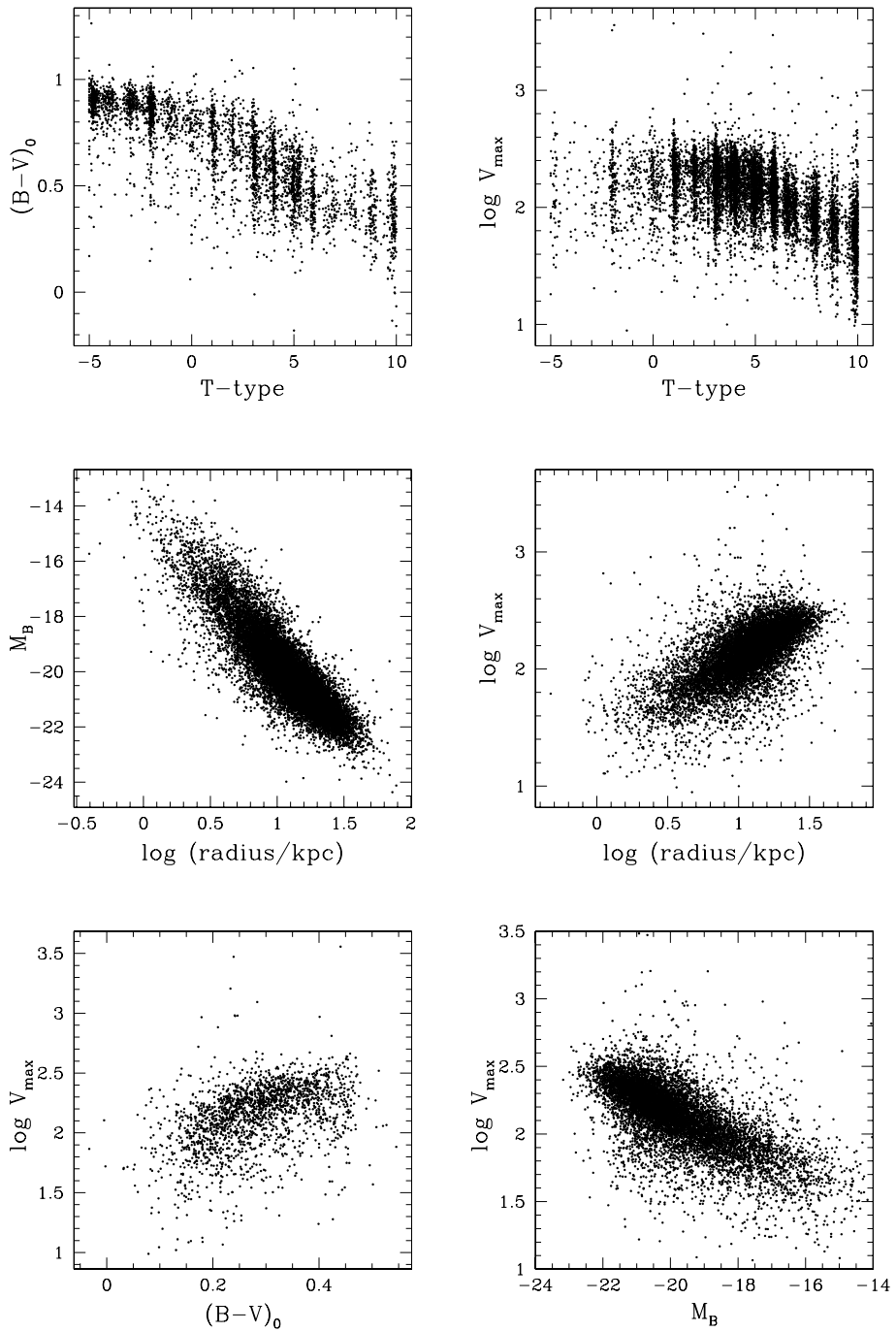


Figure 10. The strongest correlations found between the properties of the 22 000 + galaxies studied in this paper. Most of these relationships are already well known, and described for morphological subsets, such as the Tully–Fisher relation, and the size–magnitude relation. For our purposes, the most interesting trends are those of T-type with colour and V_{\max} , where considerable scatter can be seen. This is also true for the correlation between colour and V_{\max} . The scatter in these correlations is larger than the observational errors, and suggests that while morphology, colour and scale all correlate in nearby galaxies, they are still independent features.

Most of these scalings are already well known, and have been described in various contexts previously. Many become stronger when only considering certain types of galaxies (e.g. ellipticals for the Faber–Jackson, discs for Tully–Fisher). We are particularly interested here in the correlation of T-type with colour and V_{\max} (as a proxy for other scale features). Fig. 10 plots the relationship between these properties. As can be seen, later T-types are both bluer

and have lower internal velocities. These are in particular strong correlations, as shown in Table 3. As we argue in this paper, these two correlations are the reason why the Hubble sequence has been generally successful at separating galaxy types. However, as can be seen there is a large scatter in these correlations, such that at every T-type there is a wide range in colour and V_{\max} values. This is also true for the relationship between $(B - V)_0$ and V_{\max} . This diversity

cannot be accounted for by errors on classifications, or on the measured values. This shows that there are variations in colour and scale which are not accounted for by Hubble type.

6 DISCUSSION

6.1 Physical classification

For the remainder of this paper we address whether the results of the first part of this paper can be used to construct a classification system for galaxies that is physically meaningful. First, it is worth asking if we need a physical classification system for galaxies. Is it possible that relations between observables and (non-morphological) galaxy properties are enough to characterize the population? The first classification schemes by Wolf (1908), Hubble (1926), de Vaucouleurs (1959) and Sandage (1961, 1975) are purely descriptive, and the idea that a galaxy's classification should be based solely on the most obvious features seen in optical light persists (Sandage 2005). The reason given for this philosophy is that no physical understanding of what drives galaxy formation/evolution should be used to create a classification system. As Sandage (2005) explains, 'A good classification can drive the physics, but the physics must not be used to drive the classification.'

The argument of Sandage (2005), which follows Hubble's original philosophy, likely resulted from the earliest attempts to classify galaxies through the use of theoretical arguments by Jeans (1919). Hubble quite rightly avoided theory when developing his classification system, yet physical morphology does not necessarily rest upon theory, but empirical observations. Physical morphology in this sense is not a theoretical morphology. If we knew with reasonable certainty what the physical effects were that drove the properties of galaxies, a classification based on these features would be superior to theoretically, or subjectively based systems.

Several features of galaxies also make them fundamentally different from other objects which have been successfully classified based solely on their appearance, including stars, plants/animals and the chemical elements. Galaxies are fundamentally different from these types of objects as they are not stable or passive systems, nor do they have a well-defined life/death as do living organisms and stars. Furthermore, elements, plants/animals and most stars spend most of their life span in the same form. This is not the case for galaxies, where it has been shown that systems of the same mass change their appearance in optical light dramatically in the last 10 Gyr (e.g. van den Bergh et al. 2001; Conselice et al. 2005a; Ravindrinath et al. 2006). Galaxies are not static systems – they are always changing and evolving due to the complex mixtures of stars, gas, dust, dark matter and from interactions with other galaxies.

Another reason that the physical properties of galaxies can be used to devise a classification system is the fact that it is not a given that the rest-frame optical light of galaxies reveal the most important features of galaxies. For example, we now know that the bulk emission from an average galaxy is in the mid-infrared (e.g. Dale et al. 2005), and if any wavelength should be used to classify galaxies it would naturally be where most of the light is emitted. Fundamentally, if we want to classify galaxies through structure, the best approach is using a map of the distribution of mass, which would be mostly dark matter. A mapping such as this, with enough resolution for classification, does not currently exist. In blue light, where the Hubble system was and is being used, we are examining only the stars in galaxies, and often only the brightest ones, which tend to be young. This leads to physical classifications, where if we think we

understand the major properties of galaxies, we can utilize these for classification.

Knowing which properties of galaxies are not important for classification is just as critical as uncovering the dominant ones. We can understand why through analogies with other sciences. In biological taxonomy, such as separating different populations of mammals, features such as hair or eye colour, or exact size, are not classification criteria. Similarly, features such as rings, bars and even spiral arms are important for the immediate appearance of a galaxy, but these are not basic features. Classifications using these criteria are purely descriptive. Their inclusion as major classification criteria are also arbitrary, as other properties, such as the steepness of light profiles, the clumpy nature of light seen in many galaxies, the spokes and spurs seen in spiral arms, etc. were never considered important, or were technically infeasible to measure, by early morphologists.

We can use the results of this paper to construct a physically based method for classifying galaxies. Physical morphology is not a new idea, and attempts to construct a meaningful system for galaxies started with the work of Morgan (1958, 1959) who attempted to correlate 'the forms of certain galaxies and their stellar content as estimated from composite spectra' from Morgan & Mayall (1957). Later attempts include van den Bergh's (1960) study on the correlation between spiral arm structure and intrinsic brightness. Modern studies have attempted to classify ellipticals by their structures (Kormendy & Bender 1996), and at using interacting and star formation properties to classify all galaxies (e.g. Conselice 1997; Conselice, Bershady & Jangren 2000a; BJC00; Conselice et al. 2000b). As we argued in Section 5, star formation, interactions/mergers, and the masses of galaxies are the three most fundamental parameters that can be used together to form a new physical galaxy classification.

6.1.1 Mass

We concluded in Section 5 that the underlying mass (scale) of a galaxy is a fundamental property, which is responsible for the major component in our PCAs. While few would argue that the mass of a galaxy is not a fundamental criterion for classification, it is not obvious that it is possible to classify galaxies based on their mass, without direct measurements.

However, there are structural indicators in optical light which can be used as a proxy for the underlying mass in a galaxy. As shown by, for example, Graham, Trujillo & Caon (2001) and Conselice (2003) the concentration of a galaxy's light, measured through either parametrized fits to light distributions, or from direct measurements using a concentration index (BJC00), broadly correlate with the stellar and kinematic masses of galaxies. This is true at low redshift, as well as out to $z \sim 1$ (Conselice et al. 2005a).

The degree of apparent concentration of stellar light in a galaxy has been used (even if not explicitly stated) since Hubble (1926) as the main axis for nearly all galaxy classification systems. As shown in, for example, Conselice (2003) galaxy concentration relates to the bulge-to-disc ratio and Hubble type, although this breaks down for dwarfs. Furthermore, light concentration has continued as the main axis in all galaxy classification systems, such as in de Vaucouleurs (1959) and Morgan (1959), and continues as a quantitative system through fitting bulge-to-disc ratios.

While bright Hubble types generally correlate with the masses of galaxies, they do not account for other galaxy properties needed for a full classification. The fact that late-type galaxies, which generally have low masses, low bulge-to-disc ratios and low light concentrations, are blue is a result of evolutionary processes, rather than an

inherent success of the classification. It is a coincidence that Hubble types correlate well with colour in the nearby universe, as this is not the case at higher redshifts where morphologically classified ellipticals are often blue in colour and star-forming (e.g. Stanford et al. 2004; Bundy et al. 2005). This correlation breaks down even more at $z > 1$, where the Hubble sequence itself begins to dissipate.

6.1.2 Star formation

As shown in Section 5 we find a morphological dichotomy between galaxies that are dominated by recent star formation and those that are not. Our PCA reveals that colour is the major contribution to a significant principal component, which is not accounted for solely by the Hubble type, as galaxies at a given morphology type have a range of colours (Section 5.1, Fig. 10). Therefore, if we knew the current star formation rate of a galaxy it would be a very powerful classification parameter. Typically the current star formation rate is derived from either ultraviolet, $H\alpha$ or far-infrared fluxes (Kennicutt 1998), although these measurements are typically time-consuming and hard to obtain for large samples. It is therefore desirable to use a method that can estimate the star formation properties of galaxies based on optical imaging. For most galaxies, this can be done by combining colour information along with high-frequency structural features produced by young stars (Isserstedt & Schindler 1986; Conselice et al. 2000a; Conselice 2003). The clumpiness index, S (Conselice 2003) is a good measure of the unobscured current star formation rate in galaxies, and can therefore be used as an indicator.

6.1.3 Galaxy mergers/interactions

Like the scale of a galaxy and its current star formation rate, galaxy mergers and interactions are an important aspect for driving galaxy evolution. Although mergers are rarely found in the local galaxy population, they have strong effects on the evolution of galaxies and their properties. Ellipticals and high surface brightness bulges are likely the result of major mergers, and other accretion processes. In reality, all merger events for any one galaxy are nearly impossible to trace with certainty, especially old mergers that have gone through violent relaxation, after which the original orbital information is lost. Recent interactions between galaxies however will almost always have obvious signatures that will change the way galaxies appear, as well as their internal evolution, as has been shown in various methodologies.

6.2 A new classification system: the classification cube

Fig. 11 shows how galaxies of various types fit into a three-dimensional parameter space defined by galaxy mass, recent star formation, and interactions. In this diagram, the x -axis signifies the mass, while the y -axis represents the recent star formation, and the z -axis represents the degree of recent interactions with other galaxies.

As opposed to previous classification systems, the one presented in Fig. 11 can account for all the major galaxy types described in Section 2. Classical ellipticals, with little sign of recent interactions or star formation will occupy the high-mass, low star formation and low-interaction corner. The top of this classification volume also contains the S0s, dwarf ellipticals/spheroidals. S0s have little evidence for recent star formation, but are lower-mass systems than ellipticals, and they occupy the same star formation and interaction space as the ellipticals. dEs are systems with low mass, and as such

they occupy the far end of the mass sequence for these galaxies. The dwarf irregulars have a similar internal structure and mass to the dEs, except they contain star formation, and thus fall in the same mass and interaction space, but are separated in star formation space.

This system is not completely new and various aspects of it have been published in different forms. For example, van den Bergh (1976) proposed a revision of the Hubble system where S0 galaxies occupy a parallel sequence to the spirals, instead of lodged between the ellipticals and Sa galaxies as in the original Hubble sequence. The classification of van den Bergh (1976) also contains an anaemic galaxy sequence for objects with little gas. This system also classifies galaxies in terms of their bulge-to-disc ratios, making it very similar in some ways to the star formation/mass plane presented here (see Fig. 12).

LSB galaxies, as discussed earlier, have little evidence for companions or signs of interactions with other galaxies. They also have a very gradual star formation history that is still ongoing. As such they occupy the same mass sequence as the spirals, but are located on the low-interaction side of the interaction sequence.

The dichotomy between ellipticals that appear boxy and discy can also be represented by this system (Kormendy & Bender 1996), since these galaxies naturally fall along different regions of interaction and mass space. Disky ellipticals, with rotation, would have a lower mass, while the degree of boxiness correlates with the interaction history.

Other galaxies can also be classified in this system. Starbursts induced by major mergers, are placed at the high end of the interaction and star formation sequence. Galaxies undergoing violent relaxation, such as Arp 220, containing spheroidal components and step light profiles (Wright et al. 1990), would be classified towards the high-mass end of the mass sequence.

This system is constructed based on the results presented in the earlier part of this paper. Measuring the star formation, merging, and masses (either stellar or dynamical) properties of a galaxy are not trivial, but are likely to become easier in the future. We are therefore not setting out in this section a stringent method for classifying galaxies by these properties. One could do these classifications directly by measuring the star formation rate through emission lines, masses through dynamics or spectral energy distributions, and mergers/interactions through an asymmetry index or a dynamical indicator. We discuss in Section 6.3 a possible way to use the apparent morphologies of galaxies in optical light to carry out these classifications. Future work will reveal better ways of carrying out these measurements, which can then be applied for classification according to Fig. 11.

6.2.1 Other systems as projections

Other morphological systems, including physical morphological ones, can be viewed as projections of this system. The Hubble sequence, to first order, is a one-dimensional projection with the star formation and interactions collapsed on to the mass sequence. As discussed before, the Hubble sequence does not take into account these features, thus there exists a wide range of properties at each Hubble type (Roberts & Haynes 1994; Kennicutt 1998).

The colour-asymmetry diagram is a projection, in part, of the star formation, interaction sequence (Fig. 13). This is not an exact projection since the asymmetry parameter measures interactions, as well as star formation (Conselice et al. 2000a). To first order the $(B - V)_0$ colour measures the star formation history of a galaxy.

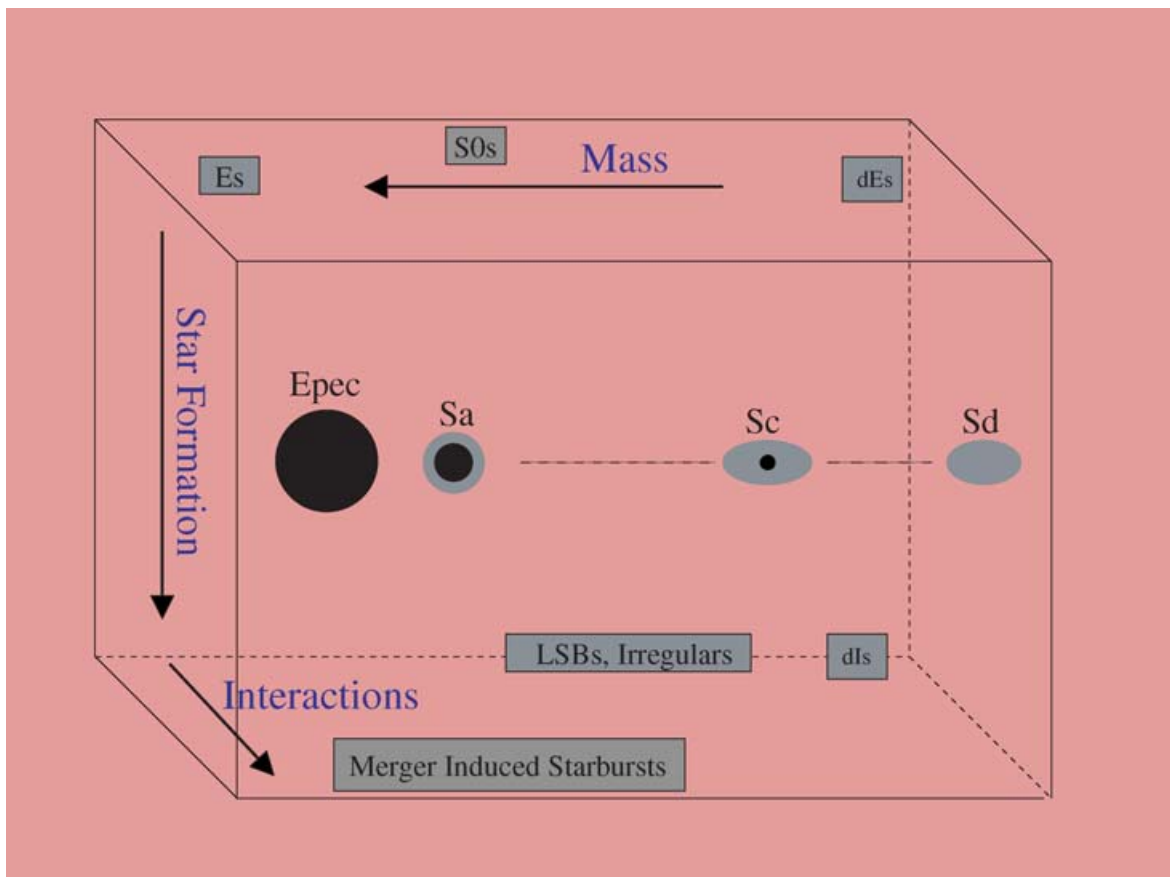


Figure 11. The three-dimensional classification volume proposed in this paper to account for all known galaxies. The three parameters used are the mass, recent star formation and interaction properties of galaxies. Several well-known galaxy types are labelled in their appropriate locations in this space. At the top of the classification cube are found galaxies with no recent star formation. Across the mass axis we progress from dEs to S0s to giant ellipticals. Any galaxies with a recent interaction/merger would be found further into the third dimension. As we go further into the cube within the y-axis, we find systems with a higher contribution of recent star formation to the stellar mass. Low-surface brightness discs would be found in a region of this space where the star formation is modestly high, and interaction history low. Merger induced starbursts are located in the high star formation, high-interaction part of the diagram, while irregulars and dIs are located towards the bottom right-hand side of the cube, as these are typically lower mass star-forming galaxies. The Hubble sequence is a one-dimensional projection of the star formation and interaction axes on to the mass sequence. This classification necessarily replaces idealized Platonic Hubble types by idealized parameters that are not always easy to retrieve, but in principle are measurable for all observable galaxies.

Galaxies with purely old stars have very red colours, while those with recent star formation are bluer. The concentration–asymmetry diagram used by BJC00 and others, is furthermore a projection of the mass–interaction sequence. More recently, Driver et al. (2006) argue that light concentration and colour are fundamental properties that separate galaxies into early- and late-types, which is again a two-dimensional projection of this new system. Likewise, Blanton et al. (2005) suggest that colour and luminosity are the most important galaxy properties, which is also shown in our analysis.

6.2.2 Idealized classifications

When Hubble invented his classification, he did so with specific examples of galaxies, however Hubble types are now thought to characterize ideal types. There are few galaxies that fit this ideal, nor is any one galaxy exactly similar to any other. This is due to the chaotic interaction and star formation history of galaxies that are, at present, not easily retrievable.

The classification system presented here replaces ideal galaxies with parameters that are in some ways idealized measurements. It

is not trivial to determine the star formation history of a galaxy, or even accurately measure its current star formation rate. Star formation does have a morphological appearance in most galaxies, the exception being systems heavily enshrouded by dust. The system presented here can still account for those galaxies, as it is very general. The method for classifying the star formation properties of a galaxy does not have to be based on morphology, but can also be done through other properties, such as fluxes at various wavelengths.

The same is true for measuring the merger history of galaxies. While many galaxies have some clues left over from merger events, these clues can be quite diverse, requiring various methods to retrieve them. Structural methods, such as the asymmetry CAS parameter (Conselice et al. 2000a,b), are useful for determining the presence of, and quantifying, current major mergers. Determining the history of past interactions is more difficult. One way is to investigate the outer parts of galaxies where the dynamical time-scales are long, and where apparently normal galaxies show evidence for past merger activity (Schweizer & Seitzer 1988). Other methods include searching for distorted H α haloes surrounding galaxies, galaxy core depletion from merging black holes (Graham 2004), and finding distorted rotation curves (Swaters et al. 1999) or line profiles (Haynes

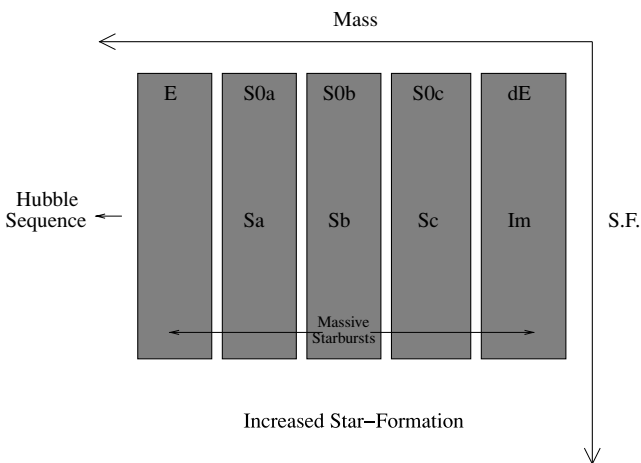


Figure 12. The system in Fig. 11 projected on to the star formation/mass plane. The Hubble sequence is labelled, and includes galaxies with a range of masses, modest star formation with no distinction made for interactions. Ellipticals, S0s, dEs and dwarf spheroidals are located at the bottom of the star formation sequence. Massive starbursts are those galaxies located at the high star formation area of this projection.

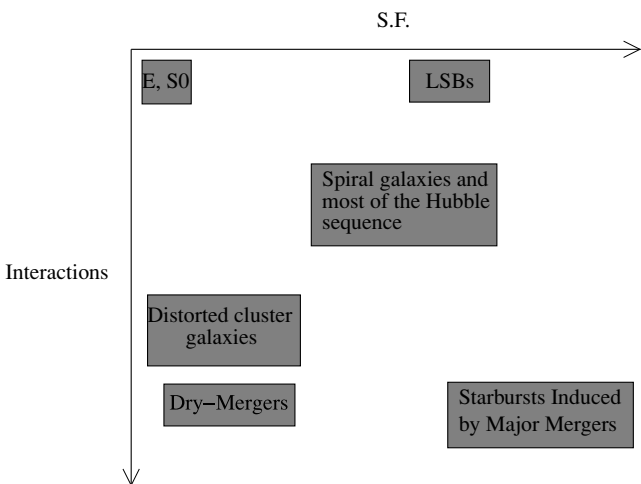


Figure 13. Projection of the star formation/interaction plane of Fig. 11. Several classes of galaxies separate along this plane perpendicular to the mass sequence. LSB galaxies are those with modest star formation and very little recent interaction history. Ellipticals and S0s are objects with relatively little star formation or interactions, and no recent interactions/mergers. Several other galaxy types, such as distorted cluster galaxies undergoing little star formation due to gas removal by the cluster, dry-mergers and starbursts induced by major mergers, are also labelled.

et al. 1998; Conselice et al. 2000b). These features are potentially all remnants of accretion, merging or interactions with other galaxies, and can in principle be used to quantify the interaction history of galaxies.

6.2.3 Unidentified galaxies?

The system presented here can classify all known galaxies, but it also has classification ‘corners’ where no nearby galaxies are known to exist, or have not been identified. One type are massive, low-interaction high star formation systems. There are plenty of galaxies that have these features at high redshift. These are likely ellipticals or discs in formation that will evolve into spheroids. For example,

systems with high mass, high star formation, and little merging could originate from gas accreted on to elliptical-like systems. Other possible galaxies not yet identified are those with various mass ranges, but low star formation and high interaction strength. Perhaps the population of distorted, but non-star-forming galaxies, or compact dwarfs found in clusters (Conselice & Gallagher 1999; Drinkwater et al. 2003) are examples of these, where the gas has been removed by the intracluster medium. Another example are the ‘dry’ mergers between spheroids with little gas (e.g. Hernandez-Toledo et al. 2006). Other possible galaxy populations can be hypothesized by studying Fig. 11.

6.3 An optical view of galaxy classification

We have argued that the three parameters – mass, star formation and interactions – can be used together to classify and trace the evolution of galaxies. These parameters have a direct correlation with the semi-irreversible processes of mass assembly or removal, and star formation where gas mass is converted into stellar mass by some conversion efficiency α . Therefore, in principle these features can be measured through stellar light distributions, which has been the primary method for classifying galaxies for nearly a century. We show in this section that this is possible. The following description follows closely the more detailed calculation given in appendix B of Conselice (2003).

We can write the initial baryonic mass of a galaxy after its initial formation ($M_{0,B}$) as

$$M_{0,B} = M_{0,S} + M_{0,G}, \quad (1)$$

where $M_{0,S}$ and $M_{0,G}$ are the initial stellar and gas masses. Over time, mass will accrete or be removed from a galaxy due to interactions and mergers. At a time T , the amount of mass added to or removed from the system, $M'(T)$ is given by

$$M'(T) = \int_0^T \dot{M}(t) dt = \int_0^T \dot{M}_S(t) dt + \int_0^T \dot{M}_G(t) dt, \quad (2)$$

with \dot{M} the mass accretion, or removal, rate as a function of time, and T is the age of the galaxy when observed. We can further divide the mass flux into stellar \dot{M}_S and gas \dot{M}_G components. Some gas will be converted into stars at each time, t , by a conversion rate, $\alpha(t)$, such that the mass converted into stars, \tilde{M}_S , is given by

$$\tilde{M}_S(T) = \int_0^T \alpha(t) M_G(t) dt, \quad (3)$$

where $\alpha(t)$ and M_G are the gas conversion rate, and gas mass as a function of time. We can then write the total stellar and gas masses as a function of time by

$$M_S(t) = M_{0,S} + \int_0^t [\dot{M}_S(t) + \alpha(t) M_G(t)] dt, \quad (4)$$

$$M_G(t) = M_{0,G} + \int_0^t [\dot{M}_G(t) - \alpha(t) M_G(t)] dt. \quad (5)$$

The three axes of our system (Fig. 11) can be represented by three terms in these equations. An interaction parameter can be represented by $M'_S(t)$, and a star formation parameter by \tilde{M}_S . We can also create dimensionless parameters that in principle correlate with measurable stellar light features. We can write the integrated interaction, $\bar{I}(t)$ and star formation $\bar{F}(t)$ strengths weighted by the final mass and time as

$$\bar{I}(t) = \int_0^T \frac{t}{T} \frac{|\dot{M}_S(t)|}{M_S(T)} dt, \quad (6)$$

$$\bar{F}(t) = \int_0^T \frac{t}{T} \frac{\alpha(t)M_G(t)}{M_S(T)} dt. \quad (7)$$

These two ideal morphological parameters are quantities that should correlate with the appearance of a galaxy, and are further elaborated in appendix B of Conselice (2003). They are weighted by time since older star formation and interactions will have less of an effect on the appearance of a galaxy. Likewise, more massive galaxies will have appearances that, in general, will be less affected by relatively lower amounts of gas converted into stars, and stars lost or gained from galaxy interactions.

What this section shows is that the main galaxy formation processes – star formation and interactions/mergers can be traced through optical light. Typically, a galaxy which has undergone recent star formation will contain clumpy light, occupied by clusters of young stars. Likewise, a galaxy undergoing a merger or interaction will appear lopsided and/or distorted in some manner. The mass of a galaxy often correlates with the light concentration, which can be estimated by eye. Therefore, by estimating the degree of disturbances, clumpy structures and how concentrated a galaxy is (i.e. bulge versus disc structures) it is possible to classify galaxies into this new system using optical light. A detailed exploration of this idea in terms of eye-ball classifications is however beyond the scope of this current paper. Quantitatively, this approach has been successfully used to classify both nearby (Conselice, Gallagher & Wyse 2002; Conselice 2003) and high-redshift galaxy populations (Conselice, Chapman & Windhorst 2003b; Conselice et al. 2004, 2005c; Grogin et al. 2005; Lehmer et al. 2005; Papovich et al. 2005; Lotz et al. 2006) within the CAS system.

7 SUMMARY AND CONCLUSIONS

This paper attempts to answer a few very basic questions about galaxies and their properties. The first is how galaxies of different morphological types are related to each other, including the relationship between various major evolutionary processes. Another question we address is whether or not the structural appearance of a galaxy contains enough information to offer this classification. To answer the first question, which constitutes the bulk of the paper, we carried out a series of statistical analyses, including PCAs, of 14 properties in 22 121 galaxies. The major results of our investigations are as follows.

(i) Spearman correlation analysis show that most measurable properties of galaxies are correlated with each other, and that Hubble types correlate strongest with stellar mass and $(U - B)_0$ and $(B - V)_0$ colour. Scale features (M_* , M_B , radius, H I gas content, far-infrared luminosity) correlate strongly with each other independent of morphological, colour or luminosity selection. Furthermore, the strong correlation between M_* and colour is independent of Hubble type.

(ii) We carry out several PCAs to determine how many PCA eigenvectors are needed to describe the major properties of all nearby galaxies. Our conclusion from this is that the major eigenvector is dominated by the scale, or mass, of a galaxy, while the next two major eigenvectors are dominated by the star formation, and galaxy interactions/mergers, respectively.

(iii) Based on points I and II, we conclude that the three major processes that should be used to classify a galaxy are: the scale or mass, interactions and mergers with other galaxies, and recent star formation.

(iv) We argue that these three features (mass, star formation and interactions) are revealed through the stellar mass distributions within galaxies. Thus the optical structure of a galaxy can be used, in principle, to accurately classify galaxies into a physically meaningful system. One way this can be done is through the CAS parameters described in Conselice (2003).

(v) Based on our analysis we present a morphological breakdown of $z \sim 0$ galaxies, including the fraction and number densities of different Hubble types (ellipticals, spirals, irregulars) at different luminosities. We find that the bulk of nearby bright galaxies with $M_B < -20$ are spirals (69 per cent), while 19 per cent are elliptical, 10 per cent S0 and 2 per cent irregular. We also investigate which types of galaxies are barred, and the number densities of barred galaxies in the nearby universe. These are intended to be useful for higher redshift comparisons, which are just now becoming possible.

In summary, this paper presents a new basic methodology for understanding and classifying galaxies. It is a physical system that uses the quantifiable parameters of mass, star formation, and interactions, and is not based on galaxy morphology. The system can account for all known galaxy types, and is a naturally outgrowth of detailed studies of galaxies over the past century. Future work on this classification scheme will include understanding the origin of the mass sequence, and why it correlates at $z \sim 0$ with star formation and bulge-to-disc ratios. Furthermore, our new classification system is by no means finalized. In the future, we will likely be able to measure galaxy masses, star formation rates and ongoing interactions with a high accuracy. Whether these measurements are done morphologically or not is irrelevant, as these three properties measured in any way can be used to classify galaxies.

ACKNOWLEDGMENTS

This work, in one way or another, has been in progress since 1995, although the bulk of it was completed and written in 2001–2002 and 2006. I thank the University of Wisconsin-Madison, the Space Telescope Science Institute, Caltech and the University of Nottingham for their support while this work was completed. An early form of Section 6 was originally included in the conclusions to my PhD thesis. I thank Jay Gallagher and Matt Bershady for their collaboration which led to many of the ideas discussed in this paper, and Alister Graham, Michael Merrifield and Sidney van den Bergh for reading and commenting on various drafts. I also thank the referee for a very constructive report with many useful suggestions. Finally, I thank Sylvia and Scott Mencner for the inspiration to produce Fig. 11. Financial support for this work was provided by the National Science Foundation through an Astronomy and Astrophysics postdoctoral Fellowship, NASA, and the UK Particle Physics and Astronomy Research Council through grants to the University of Nottingham. This research has made use of the Lyon Extragalactic Database (LEDA) and the NED which is operated by the Jet Propulsion Laboratory, California Institute of Technology, under contract with the National Aeronautics and Space Administration.

REFERENCES

- Abraham R. G., Merrifield M. R., 2000, AJ, 120, 2835
- Baldry I. K. et al., 2004, ApJ, 600, 681
- Barnes J. E., Hernquist L., 1992, ARA&A, 30, 705
- Bell E., McIntosh D. H., Katz N., Weinberg M. D., 2003, ApJS, 149, 289
- Bershady M. A., Jangren J. A., Conselice C. J., 2000, AJ, 119, 2645 (BJC00)
- Binggeli B., Sandage A., Tamman G. A., 1985, AJ, 90, 1681

- Blanton M. R., Eisenstein D., Hogg D. W., Schlegel D. J., Brinkmann J., 2005, *ApJ*, 629, 143
- Brotherton M. S., 1996, *ApJS*, 102, 1
- Bundy K., Fukugita M., Ellis R., Kodama T., Conselice C. J., 2004, *ApJ*, 601, L123
- Bundy K., Ellis R., Conselice C. J., 2005, *ApJ*, 625, 621
- Bundy K. et al., 2006, *ApJ*, 651, 120
- Buta R., Combes F., 1996, *Fund. Cosmic Phys.*, 17, 95
- Conselice C. J., 1997, *PASP*, 109, 1251
- Conselice C. J., 2003, *ApJS*, 147, 1
- Conselice C. J., 2004, in ‘Penetrating Bars Through Masks of Cosmic Dust: the Hubble Tuning Fork Strikes a New Note’, p. 489, preprint ([astro-ph/0407463](#))
- Conselice C. J., 2006, *ApJ*, 638, 686
- Conselice C. J., Gallagher J. S., 1999, *AJ*, 117, 75
- Conselice C. J., Bershadsky M. A., Jangren A., 2000a, *ApJ*, 529, 886
- Conselice C. J., Bershadsky M. A., Gallagher J. S., 2000b, *A&A*, 354, L21
- Conselice C. J., Gallagher J. S., Wyse R. F. G., 2001, *ApJ*, 559, 791
- Conselice C. J., Gallagher J. S., Wyse R. F. G., 2002, *AJ*, 123, 2246
- Conselice C. J., Bershadsky M. A., Dickinson M., Papovich C., 2003a, *AJ*, 126, 1183
- Conselice C. J., Chapman S. C., Windhorst R. A., 2003b, *ApJ*, 596, L5
- Conselice C. J., Gallagher J. S., Wyse R. F. G., 2003c, *AJ*, 125, 66
- Conselice C. J. et al., 2004, *ApJ*, 600, L139
- Conselice C. J., Blackburne J. A., Papovich C., 2005a, *ApJ*, 620, 564
- Conselice C. J., Bundy K., Ellis R. S., Brinchmann J., Vogt N. P., Phillips A. C., 2005b, *ApJ*, 628, 160
- Conselice C. J. et al., 2005c, *ApJ*, 633, 29
- Curtis H. D., 1918, *Lick Obs. Publ.*, 13, 12
- Dale D. A. et al., 2005, *ApJ*, 633, 857
- de Vaucouleurs G., 1959, *Handb. der Physik*, 53, 275
- de Vaucouleurs G., de Vaucouleurs A., Corwin H. G., Buta R. J., Paturel G., Fouque P., 1991, Third Reference Catalogue of Bright Galaxies (RC3)
- Disney M. J., 1976, *Nat*, 263, 573
- Djorgovski S., Davis M., 1987, *ApJ*, 313, 59
- Dressler A., 1980, *ApJ*, 236, 351
- Dressler A., 1984, *ARA&A*, 22, 185
- Dressler A., Lynden-Bell D., Burstein D., Davies R. L., Faber S. M., Terlevich R., Wegner G., 1987, *ApJ*, 313, 42
- Drinkwater M. J. et al., 2003, *Nat*, 423, 519
- Driver S. et al., 2006, *MNRAS*, 368, 414
- Faber S. M., 1973, *ApJ*, 179, 731
- Faber S. M. et al., 2005, *ApJ*, submitted ([astro-ph/0506044](#))
- Fall S. M., Efstathiou G., 1980, *MNRAS*, 193, 189
- Ferguson H. C., Binggeli B., 1994, *A&AR*, 6, 67
- Gallagher J. S., Hunter D. A., 1984, *ARA&A*, 22, 37
- Gallagher J. S., Hunter D. A., 1986, *AJ*, 92, 557
- Graham A. W., 2004, *ApJ*, 613, L33
- Graham A. W., Guzman R., 2003, *AJ*, 125, 2936
- Graham A. W., Trujillo I., Caon N., 2001, *AJ*, 122, 1707
- Grogan N. A. et al., 2005, *ApJ*, 627, L97
- Han M., 1995, *ApJ*, 442, 504
- Haynes M. P., Giovanelli R., 1986, *ApJ*, 306, 55
- Haynes M. P., van Zee L., Hogg D. E., Roberts M. S., Maddalena R. J., 1998, *AJ*, 115, 62
- Hernandez-Toledo H. M., Avila-Reese V., Salazar-Contreras J. R., Conselice C. J., 2006, *AJ*, 132, 71
- Holmberg E., 1958, *Lund Medd.*, II, 136
- Hubble E., 1926, *ApJ*, 64, 321
- Huchra J. P., 1977, *ApJ*, 217, 928
- Impey C., Bothun G., 1997, *ARA&A*, 35, 267
- Isserstedt J., Schindler R., 1986, *A&A*, 167, 11
- Jeans J., 1919, *Problems of Cosmogony and Stellar Dynamics*. Cambridge Univ. Press, Cambridge
- Jogee S. et al., 2004, *ApJ*, 615, L105
- Kennicutt R. C., 1998, *ARA&A*, 36, 189
- Knezek P. M., 1993, PhD thesis, Univ. Massachusetts
- Kormendy J., Bender R., 1996, *ApJ*, 464, L119
- Kuntschner H., Davies R. L., 1998, *MNRAS*, 295, L29
- Lehmer B. D. et al., 2005, *AJ*, 129, 1
- Lin L. et al., 2004, *ApJ*, 617, L9
- Lotz J. M. et al., 2006, *ApJ*, submitted ([astro-ph/0602088](#))
- Madgwick D. S. et al., 2003, *ApJ*, 599, 997
- Marzke R. O., da Costa L. N., Pellegrini P. S., Willmer C. N. A., Geller M. J., 1998, *ApJ*, 503, 617
- Mo H. J., McGaugh S. S., Bothun G. D., 1994, *MNRAS*, 267, 129
- Morgan W. W., 1958, *PASP*, 70, 364
- Morgan W. W., 1959, *PASP*, 71, 394
- Morgan W. W., Mayall N. U., 1957, *PASP*, 69, 291
- Nakamura O., Fukugita M., Yasuda N., Loveday J., Brinkmann J., Schneider D. P., Shimasaku K., SubbaRao M., 2003, *AJ*, 125, 1682
- Papovich C., Dickinson M., Giavalisco M., Conselice C. J., Ferguson H. C., 2003, *ApJ*, 598, 827
- Papovich C., Dickinson M., Giavalisco M., Conselice C. J., Ferguson H. C., 2005, *ApJ*, 631, 101
- Patton D. R., Carlberg R. G., Marzke R. O., Pritchett C. J., da Costa L. N., Pellegrini P. S., 2000, *ApJ*, 536, 15
- Pope A., Borys C., Scott D., Conselice C., Dickinson M., Mobasher B., 2005, *MNRAS*, 358, 149
- Postman M., Geller M. J., 1984, *ApJ*, 281, 95
- Ravindranath S. et al., 2004, *ApJ*, 604, L9
- Ravindranath S. et al., 2006, *ApJ*, in press ([astro-ph/0606696](#))
- Roberts M. S., Haynes M. P., 1994, *ARA&A*, 32, 115
- Romanishin W., 1986, *AJ*, 91, 76
- Sandage A., 1961, *The Hubble Atlas of Galaxies*, Carnegie Institute of Washington, Washington, DC
- Sandage A., 1975, in Sandage A., Sandage M., Kristien J., eds, *Galaxies and the Universe*. University of Chicago Press, Chicago, p. 1
- Sandage A., 2005, *ARA&A*, 43, 581
- Sandage A., Visvanathan N., 1978, *ApJ*, 223, 707
- Schweizer F., Seitzer P., 1988, *ApJ*, 328, 88
- Spitzer L., Baade W., 1951, *ApJ*, 113, 431
- Stanford S. A. et al., 2004, *AJ*, 127, 131
- Swaters R. A., Schoenmakers R. H., Sancisi R., van Albada T. S., 1999, *MNRAS*, 304, 330
- Trager S. C., Faber S. M., Worthey G., Gonzalez J. J., 2000, *AJ*, 119, 1645
- Tully R. B., Fisher J. R., 1977, *A&A*, 54, 661
- van Albada T. S., 1982, *MNRAS*, 201, 939
- van den Bergh S., 1960, *ApJ*, 131, 215
- van den Bergh S., 1966, *AJ*, 71, 922
- van den Bergh S., 1976, *ApJ*, 206, 883
- van den Bergh S., 1997, *AJ*, 113, 2054
- van den Bergh S., Cohen J. G., Crabbe C., 2001, *AJ*, 122, 611
- Whitmore B. C., 1984, *ApJ*, 278, 61
- Wirth A., Gallagher J. S., 1984, *ApJ*, 282, 85
- Wolf M., 1908, *Pub. Ap. Inst. Konig. Heidelberg*, Vol. 3, No. 5
- Worthey G., 1994, *ApJS*, 95, 107
- Wright G. S., James P. A., Joseph R. D., McLean I. S., 1990, *Nat*, 334, 417
- Zaritsky D., Rix H.-W., 1997, *ApJ*, 477, 118

This paper has been typeset from a \TeX / \LaTeX file prepared by the author.